

## Review

## Vacuum-Ultraviolet Photon Detections

Wei Zheng,<sup>1,2,\*</sup> Lemin Jia,<sup>1,2</sup> and Feng Huang<sup>1</sup>

**Vacuum-ultraviolet (VUV) photon detection technology is an effective means for the exploration in the field of space science (monitoring the formation and evolution of solar storms), high-energy physics (dark matter detection), large-scale scientific facility (VUV free electron lasers) and electronic industry (high-resolution lithography). The advancement of this technology mainly depends on the performance optimization of VUV photodetectors. In this review, we introduced the research progress on the typical VUV photodetectors based on scintillator, photomultiplier tube, semiconductor, and gas, with their unique advantages and optimal performance indicators in different applications summarized. In particular, during recent years, thanks to the advances in ultra-wide bandgap semiconductors, economical VUV photodetectors with low power consumption and small size have been encouragingly developed. Finally, we pointed out the remaining challenges for each type of VUV detector, with the aim of maximizing the performance in a variety of applications in the future.**

## INTRODUCTION

Owing to atmospheric absorption, electromagnetic waves with a wavelength range of 10–200 nm can only propagate under vacuum, thus are called vacuum-ultraviolet (VUV) light (de Oliveira et al., 2011; Pile, 2018). With the continuous development and progress of modern science and technology, VUV photon detection increasingly displays a prospect in the field of space science, basic science (high-energy physics, physical chemistry, spectral physics, etc.), electronic industry, biomedicine, environmental protection, etc.

In the field of space science, as one of the effective means of tracking stars' evolution and forecasting space weather, VUV photon detection can directly monitor changes in solar winds, which are looped out by intense activity of the sun (Baker et al., 2004; Guerrero and De Marco, 2013) (Figure 1A). Aurora, magnetic storms, and ionospheric disturbances on the earth caused by the solar winds affect human life and have done serious damage to the earth (Cane and Richardson, 2003; Gosling et al., 1978; Sibeck et al., 1991). Therefore, special photodetectors are generally needed to conduct absolute measurement of VUV photon flux under high-radiation background during all kinds of space missions, such as SOLAR (SOL-ACES and SOL-SPEC instruments) (Schmidtke et al., 2014), PROBA II (LYRA and SWAP instruments) (Hochedez et al., 2006) and Solar Orbiter (EUI and SPICE instruments) (Halain et al., 2012).

In the field of basic science, VUV photon detection plays the role of "eyes" when scientists explore the microscopic world, widely used in high-energy physics (such as detecting dark matter, Figure 1B), photo-electron spectroscopy, nonlinear optics, and surface and interface physical and chemical kinetics (Basting and Marowsky, 2005; Chini et al., 2014; Kogelschatz et al., 2000; Peng et al., 2018; Samson and Ederer, 2000; Sansone et al., 2011; Schoenlein et al., 2000; Winick and Doniach, 2012). The accuracy of various basic researches mainly depends on the accurate calibration and diagnosis of absolute light intensity for VUV radiation, such as VUV free electron laser (VUV FEL) (Ackermann et al., 2007; Grüner et al., 2007) (Figure 1C). High-performance VUV photodetectors are the key to accurate absolute calibration of radiant power.

In the field of electronic industry, technologies like the precision manufacturing of modern semiconductor devices and high-resolution lithography (such as 193, 157, and 13.5 nm lithography) have become the main driving force for VUV detectors' development (Kakizaki et al., 2004; Li et al., 2017; Richter et al., 2002; Smith and Suzuki, 2018). Precise control of the exposure dose is the key to achieving high-quality lithography, so an excellent VUV detector is required to monitor the real-time energy of single laser pulse accurately (Richter et al., 2002) (Figure 1D). In addition to all the examples above, VUV detectors also play an integral role in other VUV radiation applications such as water treatment (Kostko et al., 2008; Moussavi et al., 2014; Oppenländer, 2007) and medical imaging (Moehrs et al., 2006; Schaart et al., 2009).

---

<sup>1</sup>State Key Laboratory of Optoelectronic Materials and Technologies, School of Materials, Sun Yat-sen University, Guangzhou 510275, China

<sup>2</sup>These authors contributed equally

\*Correspondence:  
zhengw37@mail.sysu.edu.cn  
<https://doi.org/10.1016/j.isci.2020.101145>



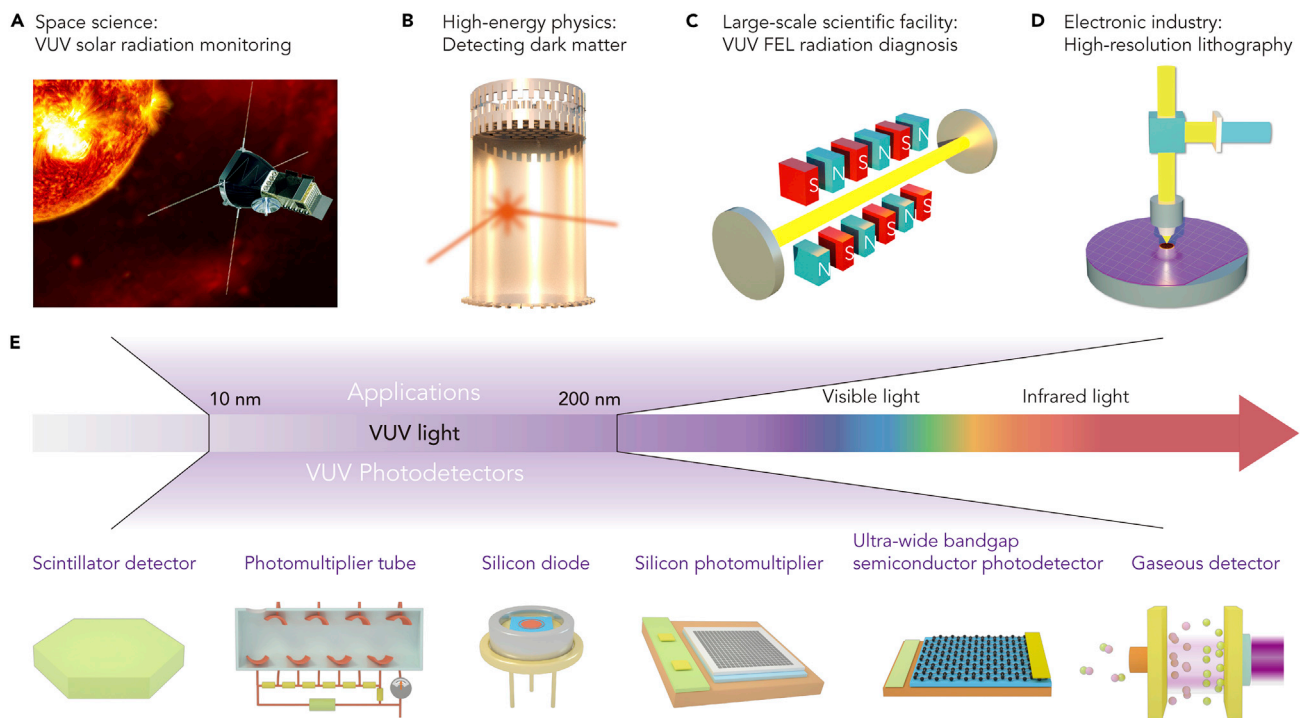


**Figure 1. VUV Photodetectors Covering a Wide Range of Applications**

(A–D) The main applications of VUV photodetectors, including VUV solar radiation monitoring (space science) (A) (reprinted with permission from Zheng et al., 2019b), detecting dark matter (high-energy physics) (B), VUV FEL radiation diagnosis (large-scale scientific facility) (C), and high-resolution lithography (electronic industry) (D).

(E) Available mainstream VUV photodetectors are presented below the electromagnetic spectrum. The device structures of scintillator, photomultiplier tube, silicon diode, silicon photomultiplier, ultra-wide bandgap semiconductor photodetector, and gaseous detector are shown in the bottom, from left to right. Note that the shape of the scintillator is arbitrary to some extent.

Generally extreme application environments present special physical and technical challenges for radiation detection in the VUV spectral range. In response to these challenges, various VUV photodetectors based on different detection media and working mechanisms have been extensively developed and researched, including scintillator detectors, photomultiplier tubes, semiconductor detectors (silicon and ultra-wide bandgap [UWBG] semiconductors) and gaseous detectors (Figure 1E). The scintillators can effectively visualize invisible VUV light by down-converting luminescence effects and perform VUV detection (Dujardin et al., 2010; Gekht et al., 2014; Sun et al., 2015) by combining with a visible light detector, which is well suited for measuring ultra-fast processes. Owing to the development of window ( $MgF_2$ ) materials, photomultiplier tube (PMT), with ultra-high sensitivity and ultra-low noise as the advantages, also become an excellent device applied to VUV detection (López Paredes et al., 2018), especially to detecting the very weak VUV radiation (Faham et al., 2015). In addition to down-conversion luminescence and light emission effects, the internal photoelectric effect of semiconductor is also used to achieve VUV detection. Silicon photodiodes, which are widely used in the visible spectrum, are also commonly used in VUV regions owing to proven manufacturing techniques (Sarubbi et al., 2006, 2008; Solt et al., 1996). The high external quantum efficiency makes it commonly used as a transfer detector standard in VUV radiation (Kuschnerus et al., 1998). Consisting of an avalanche diode array operating in Geiger mode (Eraerds et al., 2007; Jamil et al., 2018; Rethmeier, 2016), Silicon Photomultiplier (SiPM) is another photomultiplier based on silicon semiconductor technology. Owing to its insensitivity to magnetic fields, it replaces the traditional PMT in some specific applications (Moehrs et al., 2006; Schaart et al., 2009). The energy of the 200-nm VUV photons (about 6.2 eV) is close to the absorption edge (Tsao et al., 2018) of some UWBG semiconductors, such as AlN, BN, and Diamond. Therefore, UWBG semiconductor-based detectors have unique VUV selective responsiveness and excellent resistance to harsh environments compared with Si-based detectors (BenMoussa et al., 2009b; Zheng et al., 2015). In addition to the solid-state VUV detectors mentioned above, the gaseous detector, with the gas as the working medium, generates an ionization effect in which

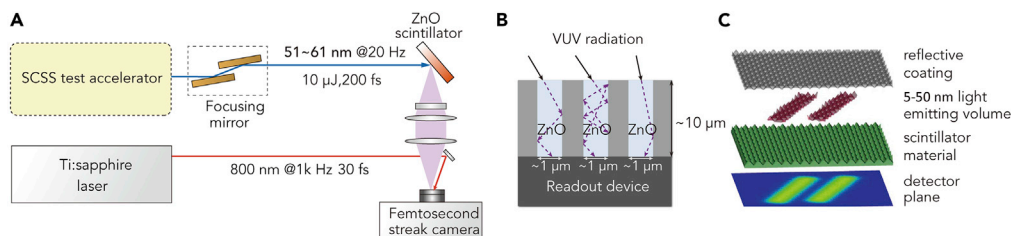


**Figure 2. Scintillators for VUV Photodetection**

(A) Schematic diagram of ultra-fast temporal resolution measurement on a ZnO scintillator responding to 51–61 nm VUV light. An experimental setup for measuring the relative jitter between a pulse from an SCSS test accelerator (XFEL prototype) and a pulse from a Ti:Sapphire laser. Reprinted with permission from Shimizu et al. (2011).  
(B) Schematic lateral illustration (not drawn to scale) of a micro/nanostructured scintillator screen made up of hydrothermally grown ZnO microrods (light blue rods/hexagons) on a porous template material. Reprinted with permission from Empizo et al. (2017).  
(C) Exploded view of the components defined in the optical model. The micro-cone scintillators are arranged in a hexagonal array with the maximum fill factor, and the modulated signal is set to two rectangular strips. The luminescence signal of the scintillation plate under VUV irradiation was detected and imaged by a spectrophotometer. Reprinted with permission from Bahrenberg et al. (2017).

the incident particles cause an output electrical signal (Richter et al., 2003; Sorokin et al., 2004) and shows a unique advantage in the field of ultra-high power VUV irradiation.

In the following parts, we will introduce the important advances reached over the past two decades in VUV photon detection technology based on scintillators, PMTs, semiconductors, and gases systematically.

### Scintillator VUV Photodetectors

Scintillators are fluorescent materials that are primarily used in the detection of high-energy (ionizing) electromagnetic and charged particle radiation. The scintillator that absorbs high-energy radiation fluoresces at a characteristic Stokes shift (longer) wavelength, which can be detected by conventional detectors such as photodiodes and PMTs. Ideal scintillators should be characterized by high light yield, high stopping power, fast scintillation response speed, and high spatial resolution. Generally, one or several performance indicators shall be upgraded according to the actual application requirements. For the time being, the most concerned scintillators that have been studied under VUV radiation include ZnO and cerium-doped yttrium aluminum garnet (Ce:YAG).

#### ZnO Scintillators for Ultra-fast VUV Photodetection

In the past two decades, the feasibility of hydrothermal-growth high-crystalline-quality ZnO (Ohshima et al., 2004; Zheng et al., 2018b) as a fast scintillator has been demonstrated (Empizo et al., 2015; Klasen et al., 2008; Nakazato et al., 2009; Tanaka et al., 2007). The emission lifetime of ZnO bulk single crystals reaches about 1.0 ns for EUV excitation at 13 nm by using Ag-plasma EUV laser and the typical emission wavelength is 380 nm. In order to further improve the temporal resolution of ZnO scintillators, deliberate doping that can introduce additional quenching channels is an effective method (Bai et al., 2014; Hao et al., 2012; Klasen et al., 2008; Shimizu et al., 2010), although it often comes at the expense of light emission intensity (Kano et al., 2011). Shimizu et al. have extensively compared the influences of different multi-ion doping on the decay time and luminous intensity of ZnO scintillators (Shimizu et al., 2011). The Fe-doped ZnO decay curve excited by the light pulse of the SCSS test accelerator fits well into a double exponential decay with a minimum time constant of 70 ps (Shimizu et al., 2010). In addition, the luminescence intensity and time decay curves appear to be independent of the excitation wavelength in the range of 50–60 nm (Yamanoi et al., 2013). ZnO scintillator doped with indium ions and a few lithium ions exhibits a single exponential decay and achieves a response time of less than 3.1 ps (Shimizu et al., 2011), making it the fastest scintillator operating below 100 nm to date. With this ultra-short response time, the relative jitter between the 200-fs pulse from the SCSS Test Accelerator and the 30-fs pulse from the Ti:Sapphire Laser can be accurately measured (Figure 2A).

Nanostructures are known to increase light emission efficiency because of quantum confinement effect (Chen et al., 2005). With the development of semiconductor nanotechnology, nanostructured ZnO scintillators growing via various methods have been further developed (Čuba et al., 2010; Empizo et al., 2014; Kobayashi et al., 2015). Empizo et al. (2017) demonstrated that the response speed of ZnO micro/nanorod scintillators could be improved without reducing the luminescence efficiency (Kwok et al., 2005; Özgür et al., 2004). In addition, the micro/nanorod scintillator (Figure 2B) enables the emitted photons to be easily guided or coupled to the readout device, effectively reducing the scattering and re-absorption probability of the scintillation signals. Therefore, it could be concluded that micro/nanostructured scintillators make efficient and accurate VUV photodetection with high temporal and spatial resolution (Angub et al., 2018) possible.

### Ce:YAG Scintillators for VUV Imaging

Ce:YAG is a scintillation crystal with high light yield and high thermal stability, often used in extreme detection conditions. Under the excitation of VUV light, the peak emission generating from the 5d-4f transition of Ce<sup>3+</sup> is located at 500–600 nm (Moszyński et al., 1994; Nishiura et al., 2011), which coincides with the sensitive spectrum of silicon photodiodes (Tang et al., 2015). Therefore, Ce:YAG is very suitable for indirect imaging in the VUV band (Booth et al., 2005).

In 2005, Kirm et al. first used VUV FEL radiation (89 nm) to study the effect of excitation density on the luminescence decay of Ce:YAG crystals at room temperature, according to which as the excitation density increases, the decay curve of the Ce:YAG crystal exhibits a non-index, indicating that the electron excitation kinetics have undergone dramatic changes (Kirm et al., 2005). For high-intensity radiation sources, the saturation effect of scintillator caused by the mutual quenching of excitons should be taken into consideration. By studying the emission saturation behaviors of Ce:YAG at different excitation wavelengths, Krzywinski et al. found that the decay kinetics of Ce<sup>3+</sup> emission was almost independent of the photon energy excited (nonlinear response) (Krzywinski et al., 2017). In addition, the structure of the scintillation crystal surface and the near layer surface may undergo irreversible changes or damages at high radiation intensity. Therefore, in order to use the scintillator in a large FEL facility safely, an accurate understanding of the threshold flux (i.e., the minimum flux that causes irreversible changes in the surface of the irradiated material) is required. Burian et al. studied the radiation resistance of Ce:YAG crystal under ultrashort laser pulse, observing that there was a damage threshold of up to  $660.8 \pm 71.2 \text{ mJ/cm}^2$  (Burian et al., 2015), which proves its feasibility for VUV imaging.

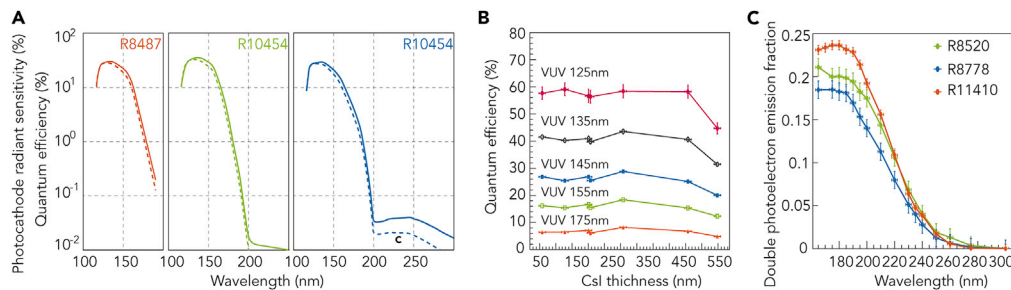
For low-intensity radiation sources, scintillators used for indirect detection have an obvious bottleneck of low sensitivity, which will aggravate the two existing problems: one is the loss of spatial resolution resulting from the divergence of scintillation light (Xu et al., 2018b); the other is the reduction of outcoupling efficiency caused by total internal reflection. To overcome the limitations above, Bahrenberg et al. designed a Ce:YAG scintillation plate composed of micro-cone structure and a coated surface with outcoupling efficiency more than four times higher than that of traditional planar scintillation plates, as shown in Figure 2C. Its unique structure, determined by the optical constants of the Ce:YAG scintillator, optimizes the directivity of images (5–50 nm) (Bahrenberg et al., 2017).

### Other Scintillators

Besides the two scintillators introduced above, there are several other scintillators having been reported based on luminous characteristics under VUV excitation. Wojtowicz et al. have committed to studying the performance and luminescence mechanism of rare-earth activated scintillators, such as BaF<sub>2</sub> (activated with Ce, Pr, Nd, Tb), YAlO<sub>3</sub> (YAP), LuAlO<sub>3</sub> (LuAP) (activated with Ce), (Lu<sub>1-x</sub>Y<sub>x</sub>)<sub>2</sub>SiO<sub>5</sub> (LYSO), and Lu<sub>1-x</sub>Y<sub>x</sub>AlO<sub>3</sub> (LuYAP, typically at 30% of Y) (activated with Ce and Pr) (Wojtowicz, 2002; Wojtowicz et al., 2000, 2006). All these scintillators have the potential to be applied to VUV detection. For example, BaF<sub>2</sub>:Ce is an extremely fast and robust scintillator material with good stopping power, excellent refractive index, and the availability of large crystals. With multiple luminescent centers, possible processes where host-to-ion energy transfer occurs are complex, which has been characterized by researchers in the way of VUV excitation spectroscopy with crucial conclusions reached. All of these efforts are critical to applying scintillators to VUV light detection at a certain wavelength or band in the future.

### VUV-Sensitive PMTs

PMTs with external photoelectric effect, owing to customizable shape, size, spectral response range (i.e., detection wavelength range), the advantages of large collection surface, and high gain, have been widely

**Figure 3. VUV Detection Performance of PMTs**

- (A) Cathode quantum efficiency of the commercial VUV PMTs: R8487, R10454, and R10825 from Hamamatsu. Reprinted with permission from Hamamatsu Photonics.
- (B) The quantum efficiency as a function of CsI thickness at different wavelengths. Reprinted with permission from Xie et al. (2012).
- (C) DPE probability for R8520, R8778, and R11410 measured as a function of incident photon wavelength. Reprinted with permission from Faham et al. (2015).

used in various analytical instruments that require high-sensitivity photodetection. PMTs are excellent candidates for VUV light detection, especially for weak VUV signals like scintillation light owing to multiplier effect. After incident light illuminates photocathode through optical window, the photoelectrons released from the photocathode are accelerated by the voltage applied to the focusing electrode and then hit on the surface of the first dynode where secondary electrons are generated. This process is repeated at all of the dynodes in PMTs, amplifying the signals more than a million times. In order to endow PMTs with selective responsivity to a certain wavelength, the window materials are often required with specific optical constants, as well as photocathode and dynode with appropriate work functions (Hamamatsu Photonics, 2007).

#### Commercial VUV PMTs

Typical commercially available PMTs with selective responsivity to VUV light are R8487, R10454, and R10825 (manufactured by Hamamatsu). Their optical windows are all MgF<sub>2</sub> with high transmittance for 120–200 nm VUV light, and the photocathodes are CsI. Figure 3A shows the cathode quantum efficiency (QE, defined as the ratio of the number of photoelectrons produced in the photocathode to that of incident photons) (Hamamatsu Photonics, 2007) of those three PMTs. The high peak QE (32.4% at 133 nm) and high suppression ratio (5,500, 121.6 nm/250 nm) indicate a supersensitive VUV photoresponse of PMTs.

#### Detection Performance of VUV PMTs

The performance of photocathodes is a key factor in determining the VUV detection capability of PMTs, with QE and aging effects being the particular concern (Singh et al., 2000). The materials currently used for VUV-sensitive photocathodes are mainly alkali halides such as CsI, CsBr, KI, and KBr and alkali tellurides such as Cs<sub>2</sub>Te, Rb<sub>2</sub>Te, Cs-K-Te, and Rb-K-Te (Zhang et al., 2017), of which CsI is the most commonly used photocathode material owing to its super-high QE (40% at 150 nm) (Breskin, 1996). Under the irradiation of VUV with different wavelengths, it has been reported that the QE of CsI is not sensitive to thickness for reflective mode (Xie et al., 2012) (Figure 3B). Tremsin et al. studied the luminescence stability of deposited and heat-treated CsI, KI, and KBr evaporation films at 115–190 nm VUV light, observing that post-evaporation heat treatment not only improved the QE of CsI and KI photocathodes but also enhanced the radiation resistance of CsI, KI, and KBr (Tremsin and Siegmund, 2000). Other studies have found that CsBr could achieve up to 35% QE (Singh et al., 2000) at 150 nm after post-evaporation heat treatment. In order to explore the radiation aging process caused by VUV, Singh et al. used angle-resolved X-ray photoelectron spectroscopy (ARXPS) to study the possible contamination and degradation of CsI photocathode under VUV irradiation (Singh et al., 2009). Surface analysis shows that, owing to the presence of lattice defects, VUV irradiation causes the CsI film to degrade layer by layer, resulting in a decrease in electron transport performance and degradation of photocurrent. The understanding of the aging mechanism proposed by this work contributes to the development and optimization of large-area photocathodes.

Moreover, with sufficient energy of incident photon, PMTs will give out a double photoelectron emission (DPE), which means two electrons will be emitted from a photonic photocathode (López Paredes et al., 2018), which is critical for PMT's calibration. For high-energy VUV incident light, the DPE probability of

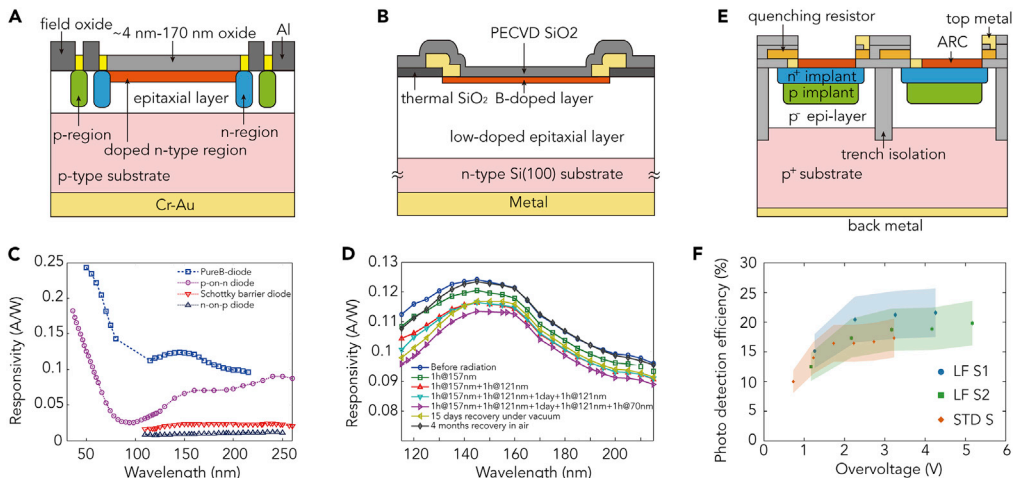


**Figure 4. Performance of Si-based VUV Photodetectors**

(A) Cross section of the AXUV/UVG Silicon photodiodes (n-p junction). Reprinted with permission from Canfield et al. (1998).

(B) Cross section of the PureB-layer diodes. Note that PECVD means plasma enhanced chemical vapor deposition. Reprinted with permission from Korde et al. (2003).

(C) Measured responsivity of four types of silicon diodes in DUV/VUV spectral range. Reprinted with permission from Shi et al. (2010a).

(D) Degradation of the VUV responsivity of a PureB-diode (with a ~10-nm native oxide layer and < 1-nm boron layer on the diode surface) after a series of VUV/DUV irradiations. Reprinted with permission from Shi et al. (2010a).

(E) Illustration of SiPM structure with trench isolation, with the correlated noise mechanisms highlighted. The trench provides “partial” optical isolation due to reflection at the interface. Reprinted with permission from Acerbi et al. (2019).

(F) PDE of VUV-HD SiPMs as a function of overvoltage. These SiPMs have low-field (LF) and standard-field (STD) versions, which differ in their doping profile. The error bars represent statistical errors, whereas the colored bands show systematic errors. Reprinted with permission from Jamil et al. (2018).

PMTs cannot be neglected (Neves et al., 2010). Faham et al. reported a series of DPE probabilities of VUV-sensitive PMTs (R11410, R8778, and R8520 from Hamamatsu) measured with varying wavelength (Figure 3C). It can be seen that the probabilities of DPE are 15%–25% in the wavelength band below 200 nm (Faham et al., 2015). Therefore, calibration of VUV PMTs for high-energy radiation with longer wavelength such as visible light should be avoided to prevent the measured QE value from being too high.

### Si-Based VUV Photodetectors

Compared with the detectors of the above types, semiconductor detectors own the advantages of small size, good compatibility, ruggedness, and ease of operation. With the most versatile and mature technology, Si-based detectors, among which silicon photodiodes and SiPMs are the representatives, are the first choice in the field of VUV detection, which faces various challenges. In the following parts, we will introduce several key issues of silicon photodiodes such as the researches and solutions to the degradation caused by external light emission and SiPMs for VUV detection during recent years.

#### Silicon Photodiode as a VUV Radiometric Transfer Standard

Silicon photodiodes provide a low-cost solution for the spatially uniform, highly linear VUV detection, and that is why they are often taken as a transfer standard for VUV radiation. For the broad-spectrum response of silicon photodiodes, VUV selective response can be achieved by applying filter material to the front surface or using a band-pass window. The basic structure of silicon photodiodes mainly contains a Schottky barrier diode, an n-p junction diode, and a p-n junction diode, among which the most common p-n junction diode protected by  $\text{SiO}_2$  has its spectral responsivity strongly degraded under VUV irradiation (Durant and Fox, 1995). This degradation is usually due to the formation of charge carrier traps (Korde and Geist, 1987; Shaw et al., 2005) in oxide passivation layer or oxide/silicon interface region. To solve this problem, n-p junction photodiodes are developed (Canfield et al., 1998; Richter et al., 2002) (e.g., AXUV, UVG, see Figure 4A) in which the positive charge in the oxide increases the surface charge collection efficiency (Kjornrattanawanich et al., 2006). Besides, the front-illuminated Pt Si-n-Si Schottky barrier photodiodes for VUV

spectral range have been developed (Solt et al., 1996). Although the existence of metal capping layers causes a low response (less than 0.05 A/W at 193 nm), it does achieve excellent optical performance stability by preventing VUV-induced ionization of detector surface. For all types of silicon photodiodes above, Kuschnerus et al. tested their radiation properties such as spectral response, radiation damage, and spatial uniformity in the spectral range of 120–600 nm, observing that only Pt Si-n-Si Schottky diodes did not show any radiation degradation, which is the biggest obstacle for silicon photodiodes being transfer detector standards (Kuschnerus et al., 1998). In order to deeply figure out the factors of radiation damage, various types of silicon diodes have been extensively tested and studied (Korde et al., 2003; Scholze et al., 2003; Shaw et al., 2005).

Aimed at achieving both high responsivity and high radiation hardness, a “pure boron” technique (Sarubbi et al., 2006, 2008) (i.e., a boron-doped p-n junction diode with no oxide passivation layer, Figure 4B) based on chemical vapor deposition (CVD) gradually develops. This method achieves a stable and steep monotonic doping profile, which extends the electric field to the surface and increases the device’s sensitivity to VUV radiation significantly. Shi et al. have been committed to the research of p<sup>+</sup>-n silicon photodiodes based on pure boron technique for a long time (Shi et al., 2009, 2010a, 2010b, 2011, 2012, 2013). The optical performance and stability in VUV spectral range of the PureB diodes have been evaluated, showing great sensitivity on the order of 0.1 A/W over the entire VUV range compared with other types of silicon diodes (Shi et al., 2010a, 2010b, 2011) (Figure 4C). Figure 4D shows the responsivity degradation of Pure B diodes under different VUV irradiation conditions, demonstrating good radiation stability (Shi et al., 2010a). Furthermore, the suitability of Pure B diodes in lithography industry has been studied (Shi et al., 2009, 2012, 2013), which achieves a responsivity of ~0.27 A/W at 13.5 nm (Shi et al., 2012). The excellent radiation hardness and the full compatibility with standard Si-based integrated circuit processing confirm the superiority of Pure B diodes in VUV detection applications. In order to further improve device performance and applicability, Mohammadi et al. studied the temperature dependence of the kinetics of Pure B CVD deposition on the patterned Si/SiO<sub>2</sub> surface (Mohammadi et al., 2014) and the robustness of the device during the integrated heat treatment step in CMOS (Nanver et al., 2014), which provides some precautions to reduce parasitic B deposition on the oxide surface and an executable solution for Pure B diodes for CMOS integration. In general, silicon-based detectors are always considered advantageous in terms of economic cost, production, and integration process. It should be emphasized that extreme high-purity wafer cleaning, proper annealing treatment, and meticulous electrode deposition are all essential elements for obtaining a high-performance detector.

#### *SiPMs with Spectral Sensitivity Optimized for VUV Detection*

SiPMs are single photon detection arrays consisting of a number of avalanche photodiodes operating in Geiger mode (Buzhan et al., 2003). Compared with traditional PMTs, SiPMs are featured by low bias voltage, insensitivity to magnetic fields, and compact structure (Musienko, 2009). Photon detection efficiency (PDE) is the most critical performance indicator for SiPMs. In recent years, the PDE of SiPMs has been significantly improved by different methods, such as reducing noise (Acerbi et al., 2015; Asano et al., 2018) and developing high-density (HD) cell with both small size and high filling factor (Acerbi et al., 2017; Sul et al., 2013).

Generally, the working band of SiPMs is about 300–1,000 nm with spectral response peak located at about 400–500 nm. In order to improve SiPMs’ sensitivity to VUV light, a few optimization methods have been proposed, including the use of wavelength shifters and anti-reflective coating, as well as the design of appropriate device structures (Bonesini et al., 2018). Figure 4E shows the typical structure of an n/p-junction SiPM, which is electrically isolated using deep trench (Acerbi et al., 2019). It can be seen that, with regard to VUV light detection, SiPMs are mainly limited by two factors: one is the significant absorption of VUV light by anti-reflective coatings (ARC, SiO<sub>2</sub>, and Si<sub>3</sub>N<sub>4</sub> in general); the other is the low penetration depth of VUV photons in silicon (Zabrodskii et al., 2015). Therefore, removing the dielectric layer from the silicon that absorbs VUV photons and using weak VUV-absorption materials such as MgF<sub>2</sub> as anti-reflective coating are effective ways to increase VUV transmittance (Bonesini et al., 2018). Some works have already reported the detection performances of a series of VUV-sensitive SiPMs (Jamil et al., 2018; Rethmeier, 2016). It can be observed from Figure 4F that the PDE of VUV-HD SiPMs for 175 nm VUV light reaches more than 20%. For space applications of SiPM, the dependence of gain on ambient temperature and precise control of operating voltage should be noted (Ogasawara et al., 2017). In general, radiation damage to SiPM will result in an increase in dark count rate, but gain and resolution will not be significantly affected

(Qiang et al., 2013). Therefore, in the task that requires high radiation tolerance, a dark environment with low temperature should be considered.

### **UWBG Semiconductor VUV Photodetectors**

For some applications of VUV (such as solar physics), considering that the radiant power in the near UV and visible spectral ranges is much higher than VUV, the spectral ranges need to be strongly suppressed. Besides, photodetectors that work in the VUV spectrum region generally have to operate in ultra-high vacuum environment without any interaction or degradation in the presence of radiation. All of those requirements determine the development of UWBG semiconductors detectors. At present, emerging UWBG semiconductors such as diamond, AlN, and BN have attracted the attention of researchers owing to their high radiation resistance and selective responsivity to VUV light (Balducci et al., 2005; BenMoussa et al., 2009b; Li et al., 2006; Soltani et al., 2008). Based on these different semiconductors, considerable progress has been made in the development of VUV photodetectors with different device structures.

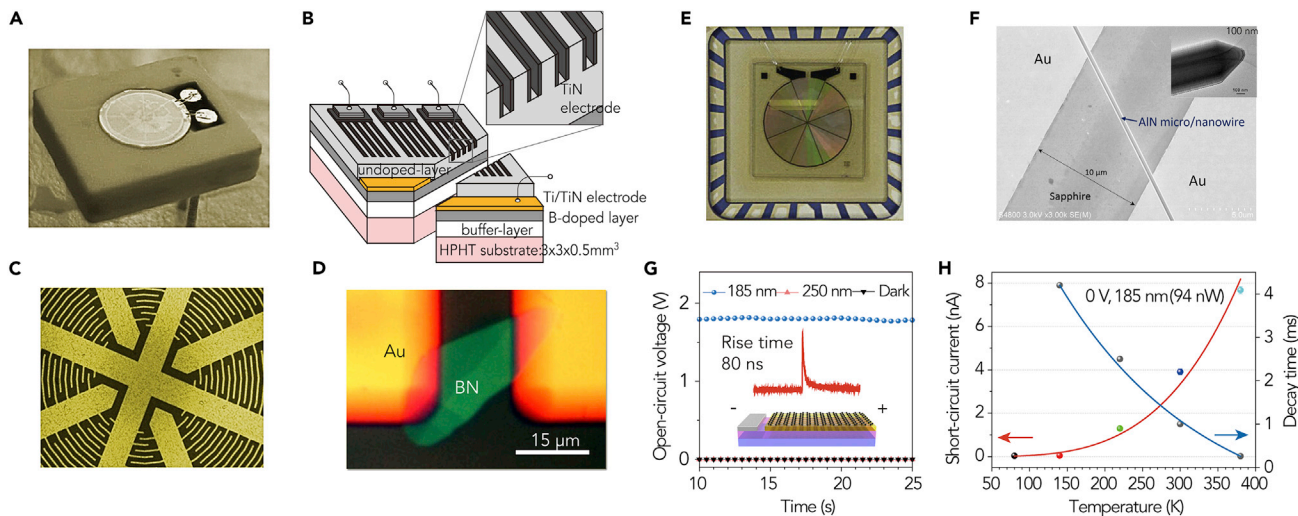
#### *Diamond VUV Photodetectors*

Owing to high thermal conductivity, small dielectric constant, and large bandgap energy ( $E_g \approx 5.5$  eV), diamond has become an ideal choice for photo-electronic applications. Moreover, diamond-based devices have been proved to be endurable for high temperature, high ionized particle flux as well as intense X-ray and VUV radiation (Alison, 2000; Fahrner et al., 2001; Hochedez et al., 2000; Monroy et al., 2003). Before 1998, attempts were made to apply natural or synthetic diamonds to VUV photodetection (Barberini et al., 2001; McKeag and Jackman, 1998). Thanks to the development of high-quality diamond single crystal growth technology (Teraji et al., 2004) and continuous optimization of device structures (Pomorski et al., 2006), the performance of diamond VUV detectors has been greatly improved. Remes et al. first reported the experimental results of VUV photoconductance and instantaneous decay of photocurrent in intrinsic CVD diamond film, which was epitaxially grown on a naturally (100) oriented diamond substrate (Remes et al., 2005). Owing to the long effective lifetime of photogenerated carriers, the typical photoresponsivity was about  $10^{-2}$  A/W at 200 nm, and the response time was less than 0.1 ms. In the same year, Balducci et al. also clarified the photoelectric detection capability of CVD single-crystal diamond in the VUV spectral region (Balducci et al., 2005). Saito et al. reported the time response, spectral responsiveness, and spatial uniformity of a photoconductive diamond detector consisting of highly oriented film, which is proved to be a candidate for VUV transfer standard detectors and energy detectors in EUV lithography (Saito et al., 2006). BenMoussa et al. (BenMoussa et al., 2004, 2006a, 2006b, 2009b) developed a series of diamond detectors including MSM type and PIN type for LYRA (Large Yield RAdiometer onboard PROBA-2) and performed a series of measurement activities by using synchrotron radiation to obtain their VUV detection performance (responsiveness, linearity, stability, homogeneity). These detectors exhibit a high photoresponse in the VUV region and differ by more than five orders of magnitude between 200 and 550 nm (BenMoussa et al., 2006b). Figure 5A is a photograph of a metal-semiconductor-metal (MSM) diamond photodetector (MSM24-R) mounted in a ceramic package (BenMoussa et al., 2009b), which has been applied in (LYRA) (BenMoussa et al., 2009a), a VUV solar radiometer. It provides solar radiation data in four UV bands with a temporal resolution of up to 10 ms. Figure 5B is a schematic diagram of a diamond VUV detector based on avalanche multiplication, which was fabricated with high-quality undoped and B-doped homoepitaxial CVD diamond layers as well as TiN thin-film electrodes. The detector achieves a responsivity of 0.325 A/W (30V, 210 nm) and a decay time of ~1.2 ms (Iwakaji et al., 2009). With the technology of high-quality diamond growth developing continuously, many remarkable results have also been achieved for VUV detectors. However, the effective doping technology of diamond still needs further breakthroughs.

In recent years, in order to improve the light absorption efficiency and carrier transmission efficiency of traditional diamond detectors, efforts have been made in developing new device structures, including the use of electrodes of different materials, the design of electrodes of different shapes and sizes, and the construction of three-dimensional devices (Iwakaji et al., 2009; Lin et al., 2018; Liu et al., 2016, 2017; Shi et al., 2016). The response peak is generally located at 210–220 nm, and the best photoresponsivity reported recently is 21.8 A/W (218 nm, at 50 V bias), achieved in an all-carbon diamond-based photodetector designed by Lin et al. (Lin et al., 2018).

#### *c-BN and h-BN VUV Photodetectors*

Boron nitride (BN) belongs to the III-V compound group and has two common structures of cubic type (c-BN,  $E_g \approx 6.2$  eV) and hexagonal type (h-BN,  $E_g \approx 6.0$  eV). c-BN manifests a series of extreme properties

**Figure 5. Typical UWBG Semiconductor-Based VUV Photodetectors**

- (A) Photograph of an MSM-structured diamond photodetector mounted in a ceramic package. Reprinted with permission from BenMoussa et al. (2009b).  
 (B) Schematic diagram of a diamond VUV detector based on high-quality undoped and B-doped homoepitaxial CVD diamond layers as well as TiN thin-film electrodes. Reprinted with permission from Iwakaji et al. (2009).  
 (C) Enlarged SEM image of the circular interdigitated electrodes of c-BN detector at the central region. Reprinted with permission from Soltani et al. (2008).  
 (D) Image of a few-layered h-BN prototype detector (thickness of ~18 nm). Reprinted with permission from Zheng et al. (2018c).  
 (E) Circular MSM-structured AlN detector (4.3 mm in diameter) installed in the ceramic package with a removable glass protection component. Reprinted with permission from BenMoussa et al. (2013).  
 (F) SEM image of the AlN micro/nanowire-based photodetector. Reprinted with permission from Zheng et al. (2015).  
 (G) Voltage output characteristics of the photovoltaic detector under different illumination conditions. When illuminated under 250 nm light, the device shows no open-circuit voltage output, so does it under dark state. Inset: Temporal-dependent VUV photoresponse and a schematic diagram of the VUV photovoltaic device structure. Reprinted with permission from Zheng et al. (2018a).  
 (H) Temperature-dependent short-circuit photocurrent and decay time at bias of 0 V. Reprinted with permission from Zheng et al. (2018b).

similar to or even better than those of diamond, including high atomic density, hardness, and thermal conductivity, and diamond has been proved as the best substrate for the heteroepitaxial growth of c-BN in VUV photodetectors (Zhang et al., 2005a, 2005b). The growth of c-BN faces many challenges such as disordered orientation caused by non-cubic BN interlayer, film thickness limitation, poor crystallinity, and poor adhesion to the substrate. Therefore, how to grow the high-quality materials is still a key factor hindering the development of c-BN-based VUV detectors. Soltani et al. fabricated a c-BN film-based VUV photodetector on a diamond-coated silicon substrate (Figure 5C), which is deposited by an electron cyclotron resonance microwave plasma CVD system with the help of He-Ar-N<sub>2</sub>-BF<sub>3</sub>-H<sub>2</sub> mixture gas (Soltani et al., 2008). Under the bias voltages of -20, -30, and -35 V, the maximum spectral responsivity at about 180 nm is 12, 23, and 32 mA/W, respectively. Also, the measured rejection ratio (180 nm/250 nm) exceeds four orders of magnitude, suggesting that the c-BN-based VUV photodetectors are able to directly detect VUV and eliminate any visible light and mid-ultraviolet noise.

h-BN, a van der Waals crystal with excellent long-term stability and electric insulation, has stronger interaction with light compared with transitional bulk crystals (Grant et al., 2016). In recent years, 2D h-BN has attracted considerable attention in the field of VUV detection owing to its low-dimensional conductive channels for fast carrier collection and high surface density of trap states for high photocurrent gain (Zheng et al., 2018c). Atomic-level h-BN nanosheets for the construction VUV detectors can be fabricated by various methods such as metal organic chemical vapor deposition, short-pulse plasma beam deposition, and ion beam sputtering deposition (Aldalbahi and Feng, 2015; Li et al., 2012; Meng et al., 2015; Rivera et al., 2017; Sajjad et al., 2014; Wang et al., 2015, 2017; Zhou et al., 2016). Liu et al. (2018) prepared high-quality h-BN by reducing the density of boundary defects and then fabricated a deep UV photodetector with the cut-off wavelength of about 225 nm and the rise and decay time of 0.32 and 0.63 s. In order to further improve the responsivity and response time, a few-layer h-BN VUV detector based on mechanical stripping was constructed (Figure 5D) and its performance was measured by synchrotron radiation (Zheng et al., 2018c). The trap centers on the surface of 2D layered h-BN can capture photogenerated carriers,

helping form an additional electronic transmission channel to generate continuous photocurrent. Owing to the contribution of persistent photoconductivity to photocurrent, the responsivity of the device is up to 2.75 A/W at 20 V bias and the corresponding external quantum efficiency (EQE) is as high as 2,133% under very weak VUV irradiation of 160 nm (3.25 pW). In addition, its VUV photodetection remains stable with temperature ranging from 80 to 580 K, which is quite suitable for extreme space environment. Recently, h-BN-based PIN heterojunction van der Waals photovoltaic VUV detector has been reported. At 0 V bias, the device exhibits ultrafast response time of 680 ns, which is two to three orders of magnitude faster than that of photoconductive h-BN photodetectors (Zheng et al., 2019a).

#### AlN Photoconductive VUV Photodetectors

AlN is another UWBG semiconductor that has both UV luminescence (Chang et al., 2019; Wei et al., 2020) and VUV light detection potential in III-V nitrides. Its direct bandgap of 6.2 eV corresponds to the cut-off edge of VUV (200 nm), indicating a perfect VUV selective responsivity. In addition, superior radiation resistance and high thermal and chemical stability (Onuma et al., 2010) also make it an ideal material for VUV photodetectors. Although p-type doping of AlN is still difficult to be achieved, the growth of AlN crystals with a low defect concentration is of primary importance. Since 2002, it has been found that AlN epitaxial films with high optical quality can be grown on sapphire by metal organic chemical vapor deposition (MOCVD) (Li et al., 2002, 2003; Nam et al., 2003; Zhang et al., 2002). Li et al. fabricated a VUV photodetector based on high-quality un-doped AlN film, with VUV/visible suppression ratio of more than four orders of magnitude and a sharp cutoff wavelength of 207 nm (Li et al., 2006). Based on the work of Li et al., Ben-Moussa et al. studied the effect of photoemission current on the output signals and came to the conclusion that, when the AlN MSM detector is operated under positive high bias voltage, the output signal would be maximized while the probability of electron escape would be reduced at the same time (BenMoussa et al., 2008).

In space application, the optical components of detectors are usually exposed to solar radiation directly, so ionization and atomic displacement damage effects are always the main reasons for space devices and instruments' degradation. In order to prove AlN-based photodetectors' universal applicability for space VUV detection, BenMoussa et al. fabricated a large-area circular MSM structured photoconductive detector that was mounted in a ceramic package with a removable glass protective component (BenMoussa et al., 2013) (Figure 5E). After exposure to protons with 14.4 MeV, no significant reduction in the detector performance was observed, and the high rejection ratio was about five orders of magnitude between 200 and 450 nm, which means that it could meet the strict requirement of filter-less VUV solar observation. In 2013, Tsai et al. also fabricated an MSM photodetector by depositing the AlN film on Si (100) substrates, which showed high temperature resistance and radiation tolerance for harsh environments (Tsai et al., 2013).

Compared with traditional bulk and thin film structured semiconductors, nanostructured ones have the advantage of strong self-exclusion effect of impurities, which makes internal defect-free possible (Alivisatos, 1997). Also, owing to their quantum confinement effect on carriers (Fang et al., 2009; Li et al., 2010; Liu et al., 2009), low-dimensional nanostructured photodetectors often have higher responsivity and/or fast response speed. In order to fabricate low-dimensional AlN photodetectors, Zheng et al. (2015) made a breakthrough of growing high-quality and inner defect-free AlN micro/nanowires through a two-step physical vapor transfer method (Figure 5F). In addition to the expected low dark current and fast response (rise time and decay time less than 0.1 and 0.2 s, respectively, limited by the measurement at that time), the detector showed a cut-off wavelength of 208 nm and manifested a significant photocurrent gain when the incident light energy exceeded the threshold of 200 nm (6.2 eV).

#### AlN Photovoltaic VUV Photodetectors

The photovoltaic detectors cannot achieve ultra-high responsivity owing to the absence of gain mechanism, but their advantage is that they can operate without bias and thus reduce power consumption. Also, owing to the separation of photogenerated carriers by built-in electric field, photovoltaic devices can achieve ultra-fast response speed (Yu and Wang, 2010). Recently, our group has revealed that the transmittance of graphene (Gr) is as high as 96% in VUV band (Zheng et al., 2018a), which could be attributed to the single atomic layer of graphene as well as its weak resistance to electromagnetic waves (Kim et al., 2009). In addition, the high carrier mobility and good conductivity of graphene (Ruoff, 2008) also make it an ideal choice for transparent electrodes in VUV detectors. Based on this discovery, a heterojunction

VUV photovoltaic device (p-Gr/AlN/p-GaN) with vertical structure of PN characteristics is constructed by assembling p-type doped graphene on the un-doped AlN thin film with high crystal quality (Zheng et al., 2018a), in which p-type graphene is used as a transparent electrode (Bae et al., 2010; Li et al., 2009) to collect holes and AlN as a VUV light absorption layer to produce photogenerated carriers. The back-to-back structure of p-Gr/AlN/p-GaN adopted in the study can suppress the thermal diffusion of positive and negative carriers (Chi On et al., 2003), resulting in a lower voltage noise density, which is helpful to monitor the ultra-weak VUV signals. Under the irradiation of 185 nm monochromatic light, the electromotive force of 1.7 V is formed at both ends of the device (Figure 5G), whereas it shows no response under dark state and 254 nm illumination. What's more, the device has an encouraging ultra-short response time of only 80 ns (Zheng et al., 2018a).

Based on the work above, the physical mechanism of this sandwich-structure device is further explored. According to the classical physical model, the rise time of photodetectors mainly depends on the transit time of non-trapped photogenerated carriers' drifting to electrodes, whereas the exponential response decay mainly results from the carriers trapped by internal defects and/or surface states, namely, the "trap states," whose lifetime directly determines the decay time of photo-response. Zheng et al. found a positive temperature effect (Figure 5H) that increasing temperature can synergistically increase the response speed and the quantum efficiency of photocurrent conversion since external heating provides active energy for trapped carriers to escape and accelerates the annihilation of trap states, thereby the decay time can be reduced (Zheng et al., 2018b). For photovoltaic detectors, a larger open-circuit voltage means a larger voltage signal output and a higher external quantum efficiency. Jia et al. implemented a PIN heterojunction device with an open-circuit voltage up to 2.45 V (the highest among that of current single-junction devices) via quasi-Fermi level splitting enhanced effect, which benefits from the variable Fermi level of graphene (Jia et al., 2020). This device also exhibits excellent VUV photodetection performance (maximum responsivity = 79.6 mA/W, EQE = 56.1%, rise time ≈ 45 ns, decay time ≈ 5 μs), further illustrating the superiority of high open-circuit voltage devices. In terms of VUV imaging, a 20-pixel linear display device based on Si substrate was constructed (Zheng et al., 2019b), but it is still far from the final imaging requirements.

#### Other Semiconductor-Based VUV Photodetectors

In addition to the silicon and three common UWBG semiconductor materials described above, many wide-bandgap semiconductors such as AlGaN (Feng et al., 2018; Han et al., 2018), which are commonly used for solar-blind UV detection, and third-generation semiconductors like GaN (Pearson et al., 1999; Yoder, 1996), ZnO (Liu et al., 2000), SiC (Gottwald et al., 2018; Hu et al., 2006; Kalinina et al., 2016; Xin et al., 2005), and Ga<sub>2</sub>O<sub>3</sub> (Qin et al., 2019, 2020; Sun et al., 2018) all have the potential of VUV detection, among which, owing to the radiation resistance and unique high-temperature resistance of SiC (which can work in harsh environments up to 600°C), the detection performance of various SiC-based Schottky diodes in the entire UV range has been studied. The first Pt/4H-SiC and the first Ni/4H-SiC detectors were observed to have the highest quantum efficiency (4% and 15%) (Xin et al., 2005) at 120 and 200 nm in the VUV region, respectively. Synchrotron radiation tests in the 3- to 400-nm range demonstrates a high detection rate of the Ni/4H-SiC detector, providing an opportunity to reduce the sensitivity threshold and to detect weak signals (Hu et al., 2006). The Cr/4H-SiC Schottky detector has also been shown to have a quantum efficiency (Kalinina et al., 2016) comparable with that of a standard Si detector. Furthermore, Cr/4H-SiC photodiodes exhibit a uniformity of responsiveness above their effective surface and a linear dependence of photocurrent from incident radiant power in the 40- to 400-nm spectral range (Gottwald et al., 2018).

The research on the detection performance of the materials above in the VUV band has proved their availability, but owing to the limitation of bandgap, that is not enough to meet the requirement of only detecting the VUV light source without filter. Therefore, selecting semiconductors with a bandgap being greater than or equal to 6.2 eV (corresponding to the upper limit of the VUV wavelength) is crucial for a filter-less VUV detector. Many binary oxides and fluorides with wider band gaps have the potential to be VUV detection materials. For example, the two-dimensional MgO (~7.3 eV) has been used to fabricate VUV photoconductive detectors (Zheng et al., 2018d) owing to its lower-dimensional conductive channels for fast carrier collection and higher surface density for photocurrent gain, achieving a detection of very weak VUV light (0.85 pW) with a cutoff wavelength of 170 nm. A filterless VUV photoconductive detector based on pulsed laser deposition (PLD) of an yttrium fluoride (NdF<sub>3</sub>) film deposited on a quartz glass substrate has been developed (Ishimaru et al., 2013; Yamazaki et al., 2017). The NdF<sub>3</sub> detector shows a good VUV selective responsiveness (cutoff wavelength of 180 nm), but its response is only 69 μA/W (at 300 V bias) (Ishimaru

Material	Structure	Responsivity (A/W)	EQE (%)	Rise Time	Decay Time	Reference	
Diamond film Cutoff wavelength: 225 nm	MSM	0.027 (200 nm, 5 V)	17	< 1 ms	> 0.1 s	Remes et al., 2005	
	PIN	0.027 (200 nm, 0 V)	17	–	–	BenMoussa et al., 2006a, 2006b	
	Schottky	18 (210 nm, 23 V)	10,649	< 10 ms	–	Liao et al., 2007	
	Avalanche	0.325 (210 nm, 30 V)	1929	–	~1.2 ms	Iwakaji et al., 2009	
	MSM	0.2 (220 nm, 30 V)	113	2 μs	400 μs	Liu et al., 2015	
	MSM (3D electrode)	9.94 (220 nm, 5 V)	5,613	–	–	Liu et al., 2016	
	MSM (Graphite electrode)	21.8 (218 nm, 50V)	12,424	310 μs	330 μs	Lin et al., 2018	
c-BN film Cutoff wavelength: 198 nm	MSM	0.032 (180 nm, 35 V)	22	–	–	Soltani et al., 2008	
Few-layered h-BN Cutoff wavelength: 220 nm	MSM	0.0001 (212 nm, 20 V)	0.06	0.32 s	0.63 s	Liu et al., 2018	
	MSM	2.75 (160 nm, 20 V)	2,135	0.3 ms	14 ms	Zheng et al., 2018c	
	PIN	0.015 (185 nm, 0 V)	10	0.68 μs	650 μs	Zheng et al., 2019a, 2019b	
AlN film Cutoff wavelength: 207 nm	MSM	0.4 (200 nm, 100 V)	248	–	–	Li et al., 2006	
	MSM	0.0045 (170 nm, 30 V)	3	< 8 s	< 3 s	BenMoussa et al., 2008	
		0.0085 (75 nm, 30 V)	3				
		0.003 (115 nm, 30 V)	14				
	PIN	0.015 (185 nm, 5 V)	10		110 ms	80 ms	Tsai et al., 2013
	PIN	0.067 (195 nm, 0 V)	43		80 ns	0.4 ms	Zheng et al., 2018a
	PIN	0.04 (185 nm, 0 V)	27		4 μs	0.26 ms	Zheng et al., 2018b
	PIN	0.0796 (194 nm, 0 V)	50.96	45 ns	5 μs	Jia et al., 2020	
		0.0777 (172 nm, 0 V)	56.1				
AlN micro/nanowire	MSM	0.39 (190 nm, 50 V)	255	< 0.1 s	< 0.2 s	Zheng et al., 2015	
2D MgO Cutoff wavelength: 170 nm	MSM	1.86 (150 nm, 4 V)	1,540	1 s	1 s	Zheng et al., 2018d	
MgGaO film Cutoff wavelength: 206 nm	PIN	0.01 (185 nm, 0 V)	7	1.94 μs	0.6 ms	Dong et al., 2019	

**Table 1. Comparison of Main Performance Parameters of Representative UWBG Semiconductor-Based VUV Photodetectors**

et al., 2013). In order to obtain a certain bandgap semiconductor to meet the response requirements of a specific VUV band, mixing the growth of two semiconductors with different bandgaps is an effective way. Related work has reported that VUV photovoltaic detectors based on amorphous MgGaO (~6.0 eV) have achieved responsivity of 2 mA/W (Xu et al., 2018a) and 10 (Dong et al., 2019) on n-type GaN and n-type SiC substrates, respectively (under 185 nm radiation). In addition, a filterless VUV detector based on high-quality calcium fluoride and cesium fluoride ( $\text{Ca}_x\text{Sr}_{1-x}\text{F}_2$ ) hybrid crystals has been developed with absorbing edges from 122 to 130 nm achieved by controlling the composition ratio (Suzuki et al., 2019).

The performance of some representative VUV photodetectors mentioned above has been summarized in Table 1. On the whole, photoconductive VUV photodetectors generally have a greater responsivity, but this is often at the expense of response speed, resulting in the failure to meet some requirements for practical application. Intentional introduction of composite centers is an available method to shorten the response time. The inherent structure of photovoltaic photodetector gives it advantage in response speed. The

optimization of functional layer and the design of device structure aim to further increase the response speed for its application in fast processes such as dynamic monitoring. More specifically, the photodetector based on AlN thin films show a relatively high figure of merit, especially in the two key aspects of response speed and selective response, indicating that it is expected to be put into practice in some fields sooner.

### Gaseous VUV Detectors

Gaseous detectors have long been one of the most widely used detectors owing to their simple construction, high radiation resistance, and low cost. The basic working principle of the gas detector is that the incident radiation ionizes the gas between the high-voltage electrode and the collecting electrode, the generated electron ion drifts to the two poles under the action of the electric field, and an output pulse is generated on the collecting electrode. This basic working principle determines its inherent properties of long-term stability and long service life. The output is basically independent of the radiation dose, that is, the radiation damage can be ignored. A variety of new Gas-based detectors have been continuously developed and tested owing to the increasingly complex application of VUV photon detectors. The gaseous photo multiplier (GPM) with the photocathode like CsI and CsBr is coupled with gas electron multiplier (GEM) or thick gas electron multiplier (THGEM) to realize photon detection and imaging such as the readouts of VUV scintillators (Breskin et al., 2000; Collaboration et al., 2009; Francke et al., 2002). Gas ionization chambers have been used as standard detectors for synchrotron radiation sources (Carlson et al., 2006; Chernyshov et al., 2009), and for the new generation of high-intensity VUV-FEL radiation sources, various photon beam radiation measurement and diagnostic devices based on gas photoionization are constantly being developed and debugged (Schreiber and Faatz, 2015).

#### *Position-Sensitive Gaseous Detectors with Solid Photocathodes*

The Ring Imaging Cherenkov (RICH) technology (Alexeev et al., 2009) in the field of particle and celestial particle physics and many other applications such as large arrays of scintillators or scintillating fibers all require the photon detectors that are immune from magnetic field and with a very large photon detection area and high positioning accuracy (Breskin et al., 2000; Joram, 1999). For GPMs, owing to the advantages of single photon sensitivity and operation in a strong magnetic field, they offer an attractive solution for photon localization in very large sensitive areas and high radiant flux (Breskin et al., 2000; Dalla Torre, 2011; Francke et al., 2002), which can be a potential alternative to PMTs in some experiments. Next, we will mainly introduce some researches on different typical applications.

GPMs' photon detection efficiency depends on three factors: photocathode quantum efficiency (QE), electron backscatter (Di Mauro et al., 1996) from the photocathode to the gas, and the efficiency of the GEMs' detecting individual electrons. The materials used for VUV-sensitive photocathodes are mainly CsI and CsBr of which the QE has been introduced in the "PMT" section. For the aging problem of photocathodes in use, micro-pattern electron multipliers can greatly reduce the damage caused by avalanche ions (Giomataris, 1998; Ketzer et al., 2004). Sekiya et al. (2009) developed a VUV GMP based on CsI photocathode with GEMs and a  $\mu$ -PIC (Micro Pixel Chamber) (Nagayoshi et al., 2004; Takada et al., 2007) (Figure 6A), which showed a good single electron sensitivity (total gas gain of  $6.7 \times 10^5$ ) and a positional sensitivity (with LaF<sub>3</sub>(Nd) scintillators as VUV source) (Sekiya et al., 2009). This work demonstrates that the combination of VUV scintillator and imaging GMP can be a new type of radiation imaging detector that compensates for the low stopping power of gas radiation detectors. A position-sensitive GPM based on a cascade configuration is proposed by Lopes et al., which is composed of two THGEMs, followed by a 2D-THCOBRA (Silva et al., 2013) being operated in Ne/CH<sub>4</sub> (5%), at a pressure of 1 bar in VUV single photon mode (Lopes et al., 2013). The detector is a suitable candidate for RICH technology owing to the charge gain of  $10^6$ , the ion back flow values of about 20%, and the position resolution of less than 300  $\mu$ m. For cryogenic liquid scintillation detectors commonly used in neutrino and dark matter experiments such as LAr (liquid argon) and LXe (liquid helium) detectors (emission wavelengths of 128 and 178 nm, respectively) (Chepel and Araújo, 2013), Xie et al. studied a low-temperature THGEM-GPM based on polytetrafluoroethylene (PTFE) with a low radiation background. At 99 K and 1.1 atm, the total sub-efficiency of the GUV photon from the LAr photon is estimated to be 8.1% (the QE of the CsI photocathode is 16.8%), and the low threshold of the initial electronic detection system before the multiplication is 12 (Xie et al., 2015). Although the detector is stable at low temperatures, the low temperature also results in a lower gain of 1,508, which may be solved by increasing the number of multipliers or adding impurities to the working gas (Duval et al., 2011). Recently, Vartsky et al. introduced an on-site monitoring system for VUV photocathode response in

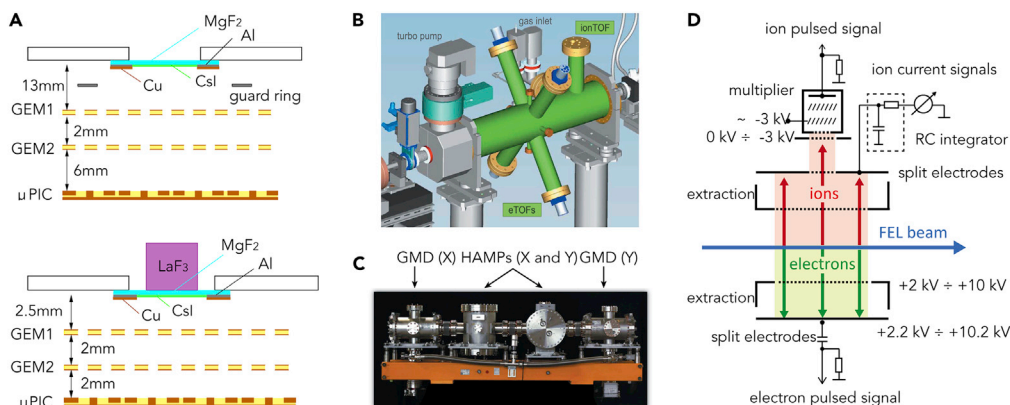


**Figure 6. Gaseous Detectors Commonly Used for VUV Detection**

(A) Schematic drawings of the VUV GMP for photon counting tests (left) and imaging tests (right). Note that LaF<sub>3</sub> is a VUV scintillator. Reprinted with permission from [Sekiya et al. \(2009\)](#).

(B) A simplified CAD model of the on-line photoionization spectrometer (OPIS) device. Reprinted with permission from [Braune et al. \(2016\)](#).

(C) A picture of the gas monitor. The left and right GMDs are used for absolute average and pulse-resolved intensity, as well as for beam position monitoring. The two HAMPs (huge-aperture open electron multipliers) in the middle measure the relative pulse-resolved intensity and beam position with the help of in-house made open electron multipliers. Reprinted with permission from [Sorokin et al. \(2019\)](#).

(D) A schematic diagram of working principle of the GMD. Reprinted with permission from [Sorokin et al. \(2019\)](#).

gas avalanche and inert liquid photon detectors, which consists of a VUV source, fiber optics, and a reference photodiode ([Vartsky et al., 2019](#)). The system allows real-time monitoring of changes in detector photosensitivity due to atmospheric conditions, impurities, or aging effects of photons and avalanches, helping researchers to design and improve detector construction and operating conditions more rationally.

#### Gas Monitor Detectors for VUV FEL

Recent advances in accelerator and precision magnetic undulator technology have enabled the construction of VUV FEL based on self-amplifying spontaneous emission (SASE) ([Ackermann et al., 2007; Ayvazyan et al., 2002, 2006](#)). Owing to the random nature of the SASE process, the photon energy of the resulting FEL pulse is always fluctuating ([Saldin et al., 2006](#)). For almost all test experiments using VUV FEL radiation, especially for studies that rely heavily on photon energy ([Neutze et al., 2000; Wabnitz et al., 2002](#)), accurate FEL photon energy of each beam is required. Therefore, a detection device that does not substantially interfere with the FEL beam is in need to feed back the real-time photon characteristics in the experiment. The peak radiant power within the FEL radiation pulse is much higher than the average power, which may saturate or even destroy solid-state detectors (such as radiation damage of silicon diodes) that are commonly used for VUV radiation measurements. In this case, the gas monitoring detector (GMD) based on the photoionization effect is the best choice for real-time monitoring of VUV FEL radiation dynamics. Over the past decade, numerous studies have shown that GMDs are a versatile tool for monitoring and conducting absolute detection of high-intensity, high-pulse VUV sources.

As early as 2003, Richter et al. developed a GMD for conducting absolute measurement of photon flux of high-intensity pulsed VUV radiation of VUV FEL, which is based on atomic photoionization of rare gases at low particle densities ([Richter et al., 2003; Sorokin et al., 2004](#)). This work measured the absolute photon number and the peak power of VUV-FEL radiation (greater than 100 MW at 87 nm) for the first time on the TESLA test equipment in Hamburg. Since the summer of 2005, Hamburg's VUV Free Electron Laser (FLASH) has been operating as a user equipment for the German Electronic Synchrotron (Deutsches Elektronen-Synchrotron, DESY) ([Ayvazyan et al., 2006](#)). For this new and complex equipment, Wellhöfer et al. proposed a method for obtaining free electron laser pulse spectrum information based on the photoionization and photoelectron spectroscopy of rare gases ([Wellhöfer et al., 2008](#)). Under the condition of low radiation and low target gas densities, detailed spectral information of the FLASH pulse can be obtained from the photoelectron spectrum of He. However, at high photon beam irradiation levels with high target

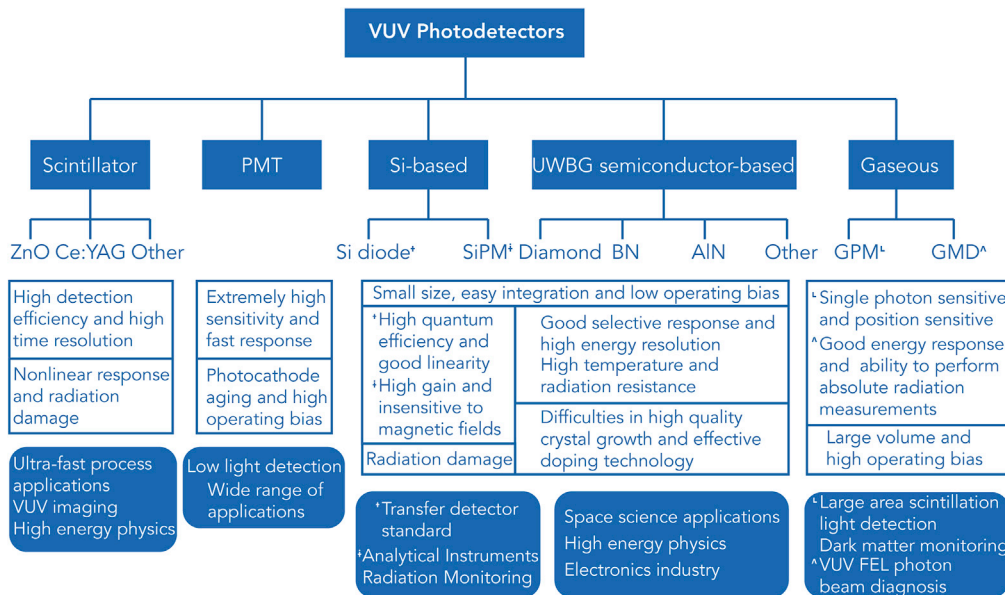


**Figure 7. Summary of All Types of VUV Photodetectors Introduced**

The main advantages (or characteristics), disadvantages (or bottlenecks), and application areas of each type of detector have been listed (from top to bottom). Note that the specific description object has been marked.

gas pressures, the Coulomb effect significantly affects the photoelectron spectrum of rare gases. This experiment uses an electronic time-of-flight (E-TOF) spectrometer (Saldin et al., 2006) to measure the photon energy of the FEL beam. In order to avoid the low count rate and high uncertainty caused by this method, the FLASH Photon Diagnostic Group developed an ion time-of-flight (I-TOF) spectrometer (Juranić et al., 2009) that utilizes the relationship between the photo-dissociation cross sections of rare gases (Tiedtke et al., 2008) to measure the photon energy of a single FEL pulse. For the new beamline FLASH2, Braune et al. reported an on-line photoionization spectrometer (OPIS) based on gas target photoionization (Figure 6B), which combines E-TOF and I-TOF with fast digitizers to achieve single-beam resolved on-line wavelength monitoring (Braune et al., 2016). With the continuous development of FLASH photon beam diagnostic devices, GMDs have become the most important diagnostic tools for measuring high-power VUV radiation intensity (Schreiber and Faatz, 2015; Tiedtke et al., 2013). Recently, a new gas monitor (Figure 6C) has been developed to measure absolute electron pulse energy (relative standard uncertainty less than 10%) and photon beam position of all existing and forthcoming FELs over a wide spectrum of VUV, EUV, and soft and hard X-ray (Sorokin et al., 2019). Figure 6D shows a schematic diagram of the detector's operation, which provides a time resolution of over 200 ns.

### Conclusion and Outlook

The urgent need to detect celestial bodies and artificial VUV radiation sources has become an important driving force for scientists to develop VUV photodetectors. To satisfy different application demands, the VUV detectors based on various media and detecting mechanisms have been widely developed. The main advantages, disadvantages, and application areas of all types of VUV photodetectors are summarized in Figure 7. Scintillators with high-time resolution (picoseconds) are usually applied to VUV detecting and imaging of ultra-fast processes, such as pulsed lasers and the pump, probe experiments related to VUV wavelength sources. In future study, the synergistic improvement between luminous efficiency and response speed is expected. The PMT with high gain and low noise is the best choice for detecting weak light, widely used in both laboratory basic sciences such as optical measuring instruments and astronomical or cosmic space researches. Therefore, solving the radiation problem of VUV-sensitive photocathodes in PMT is one expectation in the future.

With the advantages of high external quantum efficiency and mature fabrication, silicon diodes are often taken as transmission detectors' standards for VUV radiation in calibration experiments and for standard detectors in industrial field such as high-resolution lithography, with all tests having demonstrated the performance reliability of silicon diodes with new structure. With low bias, high time resolution, magnetic field

insensitivity, and compact structure, SiPM has replaced PMT in several special applications such as nuclear medicine and precision analysis. In the detection application of high-intensity VUV radiation, the increase of dark count rate caused by radiation damage is a problem waiting to be solved. During the past two decades, VUV detectors based on UWBG semiconductors developed quickly with the advantages of excellent detection performance, easy operation, miniaturization, and easy integration, gradually replacing the detectors of other types in practice. At present, many WBG semiconductors with Schottky-type device structures have achieved good performance in VUV detection. However, the inability to achieve high-quality, large-sized crystal growth and free regulation of carriers (p-type and n-type doping) remains the biggest obstacle hindering the development of VUV detectors based on WBG and UWBG semiconductors especially. For example, n-type doping of diamond and p-type doping of AlN are still hard to be achieved. Faced with this situation, actually the development of emerging low-dimensional materials has brought new possibilities for device structure design and performance optimization. At present, how to get the high-gain and high-speed avalanche detector realized is an urgent demand in the field of single-photon detection. Further work needs to be conducted for exploring the physical mechanisms of these avalanche detectors based on UWBG semiconductors and getting them better exploited.

Compared with the solid detectors mentioned above, gaseous detectors are characterized by excellent energy response and long-term stability (long service life), which can be used for absolute measurement. The combination of gas electron multiplier and VUV-sensitive photocathode provides a possible solution for photon localization over large area and high radiant flux, and the combination between gas multiplier and scintillator opens up a new, efficient way for detecting dark matter. What's more, in terms of high-intensity VUV FEL beam lines, the detection device based on gas photoionization has offered a non-destructive monitoring method. The recent expected upgradation of operating FEL sources to continuous wave (CW) requires a reassessment of gas-based diagnostic instruments. For the wavelength monitoring in high repetition rate and high photon flux multi-beam mode, the space charge accumulated in interaction region during photoionization becomes the key factor limiting performance (Braune et al., 2018).

In many application scenarios, the VUV detectors introduced above are not used alone. It is necessary to maximize each one's performance in one complex detection system based on their own characteristics to achieve overall performance optimization. For VUV detectors, a mature manufacturing process is the prerequisite for a successful application. In future researches, UWBG semiconductor VUV detectors still wait to be developed with growth doping technique and integration process waiting to be improved, and the VUV detection and imaging systems on the basis of UWBG semiconductors are expected to be used for imaging ultra-fast dynamic processes in solar activity. In response to the various problems and challenges above, researchers still need further study and exploration.

## ACKNOWLEDGMENTS

F.H and W.Z. gratefully acknowledge financial support from the National Natural Science Foundation of China (NSFC) (61427901, 61604178, 91333207, U1505252).

## AUTHOR CONTRIBUTIONS

W.Z. and F.H. provided an outline and guided writing. L.J. wrote the manuscript and prepared the figures.

## DECLARATION OF INTERESTS

The authors declare no competing interests.

## REFERENCES

- Acerbi, F., Ferri, A., Zappala, G., Paternoster, G., Picciotto, A., Gola, A., Zorzi, N., and Piemonte, C. (2015). NUV silicon photomultipliers with high detection efficiency and reduced delayed correlated-noise. *IEEE Trans. Nucl. Sci.* 62, 1318–1325.
- Acerbi, F., Gola, A., Regazzoni, V., Paternoster, G., Borghi, G., Piemonte, C., and Zorzi, N. (2017). Ultra-high Cell-Density Silicon Photomultipliers with High Detection Efficiency, Vol. 10212 (SPIE).
- Acerbi, F., Paternoster, G., Capasso, M., Marcante, M., Mazzi, A., Regazzoni, V., Zorzi, N., and Gola, A. (2019). Silicon photomultipliers: technology optimizations for ultraviolet, visible and near-infrared range. *Instruments* 3, 15.
- Ackermann, W., Asova, G., Ayvazyan, V., Azima, A., Baboi, N., Bähr, J., Balandin, V., Beutner, B., Brandt, A., Bolzmann, A., et al. (2007). Operation of a free-electron laser from the extreme ultraviolet to the water window. *Nat. Photon.* 1, 336.
- Aldalbahi, A., and Feng, P. (2015). Development of 2-D boron nitride nanosheets UV photoconductive detectors. *IEEE Trans. Electron. Devices* 62, 1885–1890.
- Alexeev, M., Birsa, R., Bradamante, F., Bressan, A., Chiosso, M., Ciliberti, P., Croci, G., Colantoni, M.L., Dalla Torre, S., Duarte Pinto, S., et al. (2009). The quest for a third generation of gaseous photon detectors for Cherenkov imaging counters. *Nucl. Instrum. Methods Phys. Res. A* 610, 174–177.

- Alison, M. (2000). Recent developments of diamond detectors for particles and UV radiation. *Semiconductor Sci. Technol.* 15, R55.
- Alivisatos, A.P. (1997). Scaling law for structural metastability in semiconductor nanocrystals. *Ber. Bunsen. Phys. Chem.* 101, 1573–1577.
- Angub, M.C.M., Vergara, C.J.T., Husay, H.A.F., Salvador, A.A., Empizo, M.J.F., Kawano, K., Minami, Y., Shimizu, T., Sarukura, N., and Somintac, A.S. (2018). Hydrothermal growth of vertically aligned ZnO nanorods as potential scintillator materials for radiation detectors. *J. Lumin.* 203, 427–435.
- Asano, A., Berge, D., Bonanno, G., Bryan, M., Gebhardt, B., Grillo, A., Hidaka, N., Kachru, P., Lapington, J., Leach, S., et al. (2018). Evaluation of silicon photomultipliers for dual-mirror small-sized telescopes of Cherenkov telescope array. *Nucl. Instrum. Methods Phys. Res. A* 912, 177–181.
- Ayyazyan, V., Baboi, N., Bähr, J., Balandin, V., Beutner, B., Brandt, A., Bohnet, I., Bolzmann, A., Brinkmann, R., Brovko, O.I., et al. (2006). First operation of a free-electron laser generating GW power radiation at 32 nm wavelength. *Eur. Phys. J. Atom Mol. Opt. Phys.* 37, 297–303.
- Ayyazyan, V., Baboi, N., Bohnet, I., Brinkmann, R., Castellano, M., Castro, P., Catani, L., Choroba, S., Cianchi, A., Dohlus, M., et al. (2002). A new powerful source for coherent VUV radiation: demonstration of exponential growth and saturation at the TTF free-electron laser. *Eur. Phys. J. Atom Mol. Opt. Phys.* 20, 149–156.
- Bae, S., Kim, H., Lee, Y., Xu, X., Park, J.-S., Zheng, Y., Balakrishnan, J., Lei, T., Kim, H.R., Song, Y.I., et al. (2010). Roll-to-roll production of 30-inch graphene films for transparent electrodes. *Nat. Nanotechnol.* 5, 574–578.
- Bahrenberg, L., Herbert, S., Mathmann, T., Danylyuk, S., Stollenwerk, J., and Loosen, P. (2017). Design of structured YAG:Ce scintillators with enhanced outcoupling for image detection in the extreme ultraviolet. *Opt. Lett.* 42, 3848–3851.
- Bai, S., Guo, T., Zhao, Y., Sun, J., Li, D., Chen, A., and Liu, C.C. (2014). Sensing performance and mechanism of Fe-doped ZnO microflowers. *Sens. Actuat. B Chem.* 195, 657–666.
- Baker, D., Kanekal, S., Li, X., Monk, S., Goldstein, J., and Burch, J. (2004). An extreme distortion of the Van Allen belt arising from the 'Hallowe'en' solar storm in 2003. *Nature* 432, 878.
- Balducci, A., Marinelli, M., Milani, E., Morgada, M.E., Tucciarone, A., Verona-Rinati, G., Angelone, M., and Pillon, M. (2005). Extreme ultraviolet single-crystal diamond detectors by chemical vapor deposition. *Appl. Phys. Lett.* 86, 193509.
- Barberini, L., Cadeddu, S., and Caria, M. (2001). A new material for imaging in the UV: CVD Diamond. *Nucl. Instrum. Methods Phys. Res. A* 460, 127–137.
- Basting, D., and Marowsky, G. (2005). *Excimer Laser Technology* (Springer Science & Business Media).
- BenMoussa, A., Schühle, U., Haenen, K., Nesládek, M., Koizumi, S., and Hochedez, J.F. (2004). PIN diamond detector development for LYRA, the solar VUV radiometer on board PROBA II. *Phys. Status Solidi* 201, 2536–2541.
- BenMoussa, A., Schühle, U., Scholze, F., Kroth, U., Haenen, K., Saito, T., Campos, J., Koizumi, S., Laubis, C., Richter, M., et al. (2006a). Radiometric characteristics of new diamond PIN photodiodes. *Meas. Sci. Technol.* 17, 913–917.
- BenMoussa, A., Theissen, A., Scholze, F., Hochedez, J., Schühle, U., Schmutz, W., Haenen, K., Stockman, Y., Soltani, A., and McMullin, D. (2006b). Performance of diamond detectors for VUV applications. *Nucl. Instrum. Methods Phys. Res. A* 568, 398–405.
- BenMoussa, A., Hochedez, J.F., Dahal, R., Li, J., Lin, J.Y., Jiang, H.X., Soltani, A., Jaeger, J.-C.D., Kroth, U., and Richter, M. (2008). Characterization of AlN metal-semiconductor-metal diodes in the spectral range of 44–360nm: photoemission assessments. *Appl. Phys. Lett.* 92, 022108.
- BenMoussa, A., Dammash, I.E., Hochedez, J.-F., Schühle, U., Koller, S., Stockman, Y., Scholze, F., Richter, M., Kroth, U., Laubis, C., et al. (2009a). Pre-flight calibration of LYRA, the solar VUV radiometer on board PROBA2. *Astron. Astrophys.* 508, 1085–1094.
- BenMoussa, A., Soltani, A., Schühle, U., Haenen, K., Chong, Y.M., Zhang, W.J., Dahal, R., Lin, J.Y., Jiang, H.X., Barkad, H.A., et al. (2009b). Recent developments of wide-bandgap semiconductor based UV sensors. *Diamond Relat. Mater.* 18, 860–864.
- BenMoussa, A., Soltani, A., Gerbedoen, J.C., Saito, T., Averin, S., Gissot, S., Giordanengo, B., Berger, G., Kroth, U., De Jaeger, J.C., et al. (2013). Developments, characterization and proton irradiation damage tests of AlN detectors for VUV solar observations. *Nucl. Instrum. Methods Phys. Res. A* 312, 48–53.
- Bonesini, M., Cervi, T., Menegoli, A., Prata, M., Raselli, G., Rossella, M., Spanu, M., and Torti, M. (2018). Detection of vacuum ultraviolet light by means of SiPM for high energy physics experiments. *Nucl. Instrum. Methods Phys. Res. A* 912, 235–237.
- Booth, M., Brisco, O., Brunton, A., Cashmore, J., Elbourn, P., Elliner, G., Gower, M., Greuters, J., Grunewald, P., and Gutierrez, R. (2005). High-resolution EUV imaging tools for resist exposure and aerial image monitoring. Paper presented at: Emerging Lithographic Technologies IX (International Society for Optics and Photonics).
- Braune, M., Brenner, G., Dzirarhyski, S., Juranic, P., Sorokin, A., and Tiedtke, K. (2016). A non-invasive online photoionization spectrometer for FLASH2. *J. Synchrotron Radiat.* 23, 10–20.
- Braune, M., Buck, J., Kuhlmann, M., Grunewald, S., Dusterer, S., Viehaus, J., and Tiedtke, K. (2018). Non-invasive online wavelength measurements at FLASH2 and present benchmark. *J. Synchrotron Radiat.* 25, 3–15.
- Breskin, A. (1996). CsI UV photocathodes: history and mystery. *Nucl. Instrum. Methods Phys. Res. A* 371, 116–136.
- Breskin, A., Boutboul, T., Buzulutskov, A., Chechik, R., Garty, E.S.G., and Singh, B.K. (2000). Advances in gas avalanche photomultipliers. *Nucl. Instrum. Methods Phys. Res. A* 442, 58–67.
- Burian, T., Hájková, V., Chalupský, J., Vyšín, L., Boháček, P., Přeček, M., Wild, J., Özkan, C., Coppola, N., Farahani, S.D., et al. (2015). Soft x-ray free-electron laser induced damage to inorganic scintillators. *Opt. Mater. Express* 5, 254–264.
- Buzhan, P., Dolgoshein, B., Filatov, L., Ilyin, A., Kantzerov, V., Kaplin, V., Karakash, A., Kayumov, F., Klemin, S., and Popova, E. (2003). Silicon photomultiplier and its possible applications. *Nucl. Instrum. Methods Phys. Res. A* 504, 48–52.
- Cane, H.V., and Richardson, I.G. (2003). Interplanetary coronal mass ejections in the near-Earth solar wind during 1996–2002. *J. Geophys. Res. Space Phys.* 108, 1156.
- Canfield, L.R., Vest, R.E., Korde, R., Schmidtke, H., and Desor, R. (1998). Absolute silicon photodiodes for 160 nm to 254 nm photons. *Metrologia* 35, 329–334.
- Carlson, S., Clausén, M., Gridneva, L., Sommarin, B., and Svensson, C. (2006). XAFS experiments at beamline I811, MAX-lab synchrotron source, Sweden. *J. Synchrotron Radiat.* 13, 359–364.
- Chang, H., Chen, Z., Li, W., Yan, J., Hou, R., Yang, S., Liu, Z., Yuan, G., Wang, J., Li, J., et al. (2019). Graphene-assisted quasi-van der Waals epitaxy on AlN film for ultraviolet light emitting diodes on nano-patterned sapphire substrate. *Appl. Phys. Lett.* 114, 091107.
- Chen, S.J., Liu, Y.C., Shao, C.L., Mu, R., Lu, Y.M., Zhang, J.Y., Shen, D.Z., and Fan, X.W. (2005). Structural and optical properties of uniform ZnO nanosheets. *Adv. Mater.* 17, 586–590.
- Chepel, V., and Araújo, H. (2013). Liquid noble gas detectors for low energy particle physics. *J. Instrum.* 8, R04001.
- Chernyshov, A., Veligzhanin, A., and Zubavichus, Y.V. (2009). Structural materials science end-station at the kurchatov synchrotron radiation source: recent instrumentation upgrades and experimental results. *Nucl. Instrum. Methods Phys. Res. A* 603, 95–98.
- Chi On, C., Okyay, A.K., and Saraswat, K.C. (2003). Effective dark current suppression with asymmetric MSM photodetectors in Group IV semiconductors. *IEEE Photon. Technol. Lett.* 15, 1585–1587.
- Chini, M., Wang, X., Cheng, Y., Wang, H., Wu, Y., Cunningham, E., Li, P.-C., Heslar, J., Telnov, D.A., Chu, S.-I., et al. (2014). Coherent phase-matched VUV generation by field-controlled bound states. *Nat. Photon.* 8, 437.
- Collaboration, T.A., Boccone, V., Lightfoot, P.K., Mavrokordidis, K., Regenfus, C., Amsler, C., Badertscher, A., Bueno, A., Cabrera, H., Carmona-Benitez, M.C., et al. (2009). Development of wavelength shifter coated reflectors for the ArDM argon dark matter detector. *J. Instrum.* 4, P06001.
- Cuba, V., Gbur, T., Můčka, V., Nikl, M., Kučerková, R., Pospíšil, M., and Jakubec, I. (2010). Properties

- of ZnO nanocrystals prepared by radiation method. *Radiat. Phys. Chem.* 79, 27–32.
- Dalla Torre, S. (2011). Status and perspectives of gaseous photon detectors. *Nucl. Instrum Methods Phys. Res. A* 639, 111–116.
- de Oliveira, N., Joyeux, D., and Nahon, L. (2011). Spectroscopy in the vacuum-ultraviolet. *Nat. Photon.* 5, 249.
- Di Mauro, A., Nappi, E., Posa, F., Breskin, A., Buzulutskov, A., Chechik, R., Biagi, S., Paic, G., and Piuz, F. (1996). Photoelectron backscattering effects in photoemission from CsI into gas media. *Nucl. Instrum Methods Phys. Res. A* 371, 137–142.
- Dong, M., Zheng, W., Xu, C., Lin, R., Zhang, D., Zhang, Z., and Huang, F. (2019). Ultrawide-bandgap amorphous MgGaO: nonequilibrium growth and vacuum ultraviolet application. *Adv. Opt. Mater.* 7, 1801272.
- Dujardin, C., Amans, D., Belsky, A., Chaput, F., Ledoux, G., and Pillonnet, A. (2010). Luminescence and scintillation properties at the nanoscale. *IEEE Trans. Nucl. Sci.* 57, 1348–1354.
- Durant, N.M., and Fox, N.P. (1995). Evaluation of solid-state detectors for ultraviolet radiometric applications. *Metrologia* 32, 505–508.
- Duval, S., Breskin, A., Budnik, R., Chen, W., Carduner, H., Cortesi, M., Cussonneau, J., Donnard, J., Lamblin, J., and Le Ray, P. (2011). On the operation of a micropattern gaseous UV-photomultiplier in liquid-Xenon. *J. Instrum.* 6, P04007.
- Empizo, M.J.F., Fukuda, K., Arita, R., Minami, Y., Yamanoi, K., Shimizu, T., Sarukura, N., Vargas, R.M., Salvador, A.A., and Sarmago, R.V. (2014). Photoluminescence properties of a single ZnO microstructure for potential scintillator applications. *Opt. Mater.* 38, 256–260.
- Empizo, M.J.F., Santos-Putungan, A.B., Yamanoi, K., Salazar, H.T., Anguluan, E.P., Mori, K., Arita, R., Minami, Y., Luong, M.V., Shimizu, T., et al. (2017). Structural and optical characterization and scintillator application of hydrothermal-grown ZnO microrods. *Opt. Mater.* 65, 82–87.
- Empizo, M.J.F., Yamanoi, K., Fukuda, K., Arita, R., Minami, Y., Shimizu, T., Sarukura, N., Fukuda, T., Santos-Putungan, A.B., and Vargas, R.M. (2015). Photoluminescence investigations of bulk and microstructured ZnO crystals for scintillator applications. *J. Ceram. Process. Res.* 16, 98–101.
- Eraerds, P., Legré, M., Rochas, A., Zbinden, H., and Gisin, N. (2007). SiPM for fast photon-counting and multiphoton detection. *Opt. Express* 15, 14539–14549.
- Faham, C.H., Gehman, V.M., Currie, A., Dobi, A., Sorensen, P., and Gaitskell, R.J. (2015). Measurements of wavelength-dependent double photoelectron emission from single photons in UV-sensitive photomultiplier tubes. *J. Instrum.* 10, P09010.
- Fahrner, W.R., Job, R., and Werner, M. (2001). Sensors and smart electronics in harsh environment applications. *Microsyst. Technol.* 7, 138–144.
- Fang, X., Xiong, S., Zhai, T., Bando, Y., Liao, M., Gautam, U.K., Koide, Y., Zhang, X., Qian, Y., and Golberg, D. (2009). High-performance blue/ultraviolet-light-sensitive ZnSe-nanobelt photodetectors. *Adv. Mater.* 21, 5016–5021.
- Feng, Z., Feng, Q., Zhang, J., Li, X., Li, F., Huang, L., Chen, H.-Y., Lu, H.-L., and Hao, Y. (2018). Band alignment of SiO<sub>2</sub>(Al<sub>x</sub>Ga<sub>1-x</sub>)<sub>2</sub>O<sub>3</sub> (0 ≤ x ≤ 0.49) determined by X-ray photoelectron spectroscopy. *Appl. Surf. Sci.* 434, 440–444.
- Francke, T., Peskov, V., Rodionov, I., and Sokolova, T. (2002). Novel position-sensitive gaseous detectors with solid photocathodes. *IEEE Trans. Nucl. Sci.* 49, 977–983.
- Gektin, A.V., Belsky, A.N., and Vasil'ev, A.N. (2014). Scintillation efficiency improvement by mixed crystal use. *IEEE Trans. Nucl. Sci.* 61, 262–270.
- Giomataris, Y. (1998). Development and prospects of the new gaseous detector "Micromegas". *Nucl. Instrum Methods Phys. Res. A* 419, 239–250.
- Gosling, J.T., Asbridge, J.R., Bame, S.J., and Feldman, W.C. (1978). Solar wind stream interfaces. *J. Geophys. Res. Space Phys.* 83, 1401–1412.
- Gottwald, A., Kroth, U., Kalinina, E., and Zabrodskii, V. (2018). Optical properties of a Cr/4H-SiC photodetector in the spectral range from ultraviolet to extreme ultraviolet. *Appl. Opt.* 57, 8431–8436.
- Grant, J.T., Carrero, C.A., Goeltl, F., Venegas, J., Mueller, P., Burt, S.P., Specht, S.E., McDermott, W.P., Chieregato, A., and Hermans, I. (2016). Selective oxidative dehydrogenation of propane to propene using boron nitride catalysts. *Science* 354, 1570–1573.
- Grüner, F., Becker, S., Schramm, U., Eichner, T., Fuchs, M., Weingartner, R., Habs, D., Meyer-ter-Vehn, J., Geissler, M., and Ferrario, M. (2007). Design considerations for table-top, laser-based VUV and X-ray free electron lasers. *Appl. Phys. B* 86, 431–435.
- Guerrero, M.A., and De Marco, O. (2013). Analysis of far-UV data of central stars of planetary nebulae: occurrence and variability of stellar winds. *Astron. Astrophys.* 553, A126.
- Halain, J.-P., Rochus, P., Renotte, E., Appourchaux, T., Berghmans, D., Harra, L., Schühle, U., Schmutz, W., Auchère, F., Zhukov, A., et al. (2012). The EUI Instrument on Board the Solar Orbiter Mission: From Breadboard and Prototypes to Instrument Model Validation, Vol. 8443 (SPIE).
- Hamamatsu Photonics, K. (2007). Photomultiplier Tubes: Basics and Applications. Edition 3a 310. URL: <https://www.hamamatsu.com/jp/en/index.html>.
- Han, W.Y., Zhang, Z.W., Li, Z.M., Chen, Y.R., Song, H., Miao, G.Q., Fan, F., Chen, H.F., Liu, Z., and Jiang, H. (2018). High performance back-illuminated MIS structure AlGaN solar-blind ultraviolet photodiodes. *J. Mater. Sci. Mater. Electron.* 29, 9077–9082.
- Hao, Y.-M., Lou, S.-Y., Zhou, S.-M., Yuan, R.-J., Zhu, G.-Y., and Li, N. (2012). Structural, optical, and magnetic studies of manganese-doped zinc oxide hierarchical microspheres by self-assembly of nanoparticles. *Nanoscale Res. Lett.* 7, 100.
- Hochdedez, J.F., Schmutz, W., Stockman, Y., Schühle, U., BenMoussa, A., Koller, S., Haenen, K., Berghmans, D., Defise, J.M., Halain, J.P., et al. (2006). LYRA, a solar UV radiometer on Proba2. *Adv. Space Res.* 37, 303–312.
- Hochdedez, J.F., Verwichte, E., Bergonzo, P., Guizard, B., Mer, C., Tromson, D., Sacchi, M., Dhez, P., Hainaut, O., Lemaire, P., et al. (2000). Future diamond UV imagers for solar physics. *Phys. Status Solidi* 181, 141–149.
- Hu, J., Xin, X., Zhao, J.H., Yan, F., Guan, B., Seely, J., and Kjornrattanawanich, B. (2006). Highly sensitive visible-blind extreme ultraviolet Ni/4H-SiC Schottky photodiodes with large detection area. *Opt. Lett.* 31, 1591–1593.
- Ishimaru, T., Ieda, M., Ono, S., Yokota, Y., Yanagida, T., and Yoshikawa, A. (2013). Vacuum ultraviolet photoconductive detector based on pulse laser deposition-grown neodymium fluoride thin film. *Thin Solid Films* 534, 12–14.
- Iwakaji, Y., Kanasugi, M., Maida, O., and Ito, T. (2009). Characterization of diamond ultraviolet detectors fabricated with high-quality single-crystalline chemical vapor deposition films. *Appl. Phys. Lett.* 94, 223511.
- Jamil, A., Ziegler, T., Hufschmidt, P., Li, G., Lupin-Jimenez, L., Michel, T., Ostrovskiy, I., Retière, F., Schneider, J., and Wagenpfel, M. (2018). VUV-sensitive silicon photomultipliers for xenon scintillation light detection in nEXO. *IEEE Trans. Nucl. Sci.* 65, 2823–2833.
- Jia, L., Zheng, W., Lin, R., and Huang, F. (2020). Ultra-high photovoltage (2.45 V) forming in graphene heterojunction via quasi-fermi level splitting enhanced Effect. *iScience* 23, 100818.
- Joram, C. (1999). Large area hybrid photodiodes. *Nucl. Phys. B Proc. Suppl.* 78, 407–415.
- Juranić, P.N., Martins, M., Viehhaus, J., Bonfigt, S., Jahn, L., Ilchen, M., Klumpp, S., and Tiedtke, K. (2009). Using I-TOF spectrometry to measure photon energies at FELs. *J. Instrum.* 4, P09011.
- Kakizaki, K., Fujimoto, J., Yamazaki, T., Suzuki, T., Matsunaga, T., Kawasaji, Y., Watanabe, Y., Kaminishi, M., Inoue, T., Mizoguchi, H., et al. (2004). Development of High-Power ArF/F2 Laser Platform for VUV Microlithography, Vol. 5377 (SPIE).
- Kalinina, E.V., Violina, G.N., Belik, V.P., Nikolaev, A.V., and Zabrodskii, V.V. (2016). Quantum efficiency of 4H-SiC detectors within the range of 114–400 nm. *Tech. Phys. Lett.* 42, 1057–1059.
- Kano, M., Wakamiya, A., Sakai, K., Yamanoi, K., Cadatal-Raduban, M., Nakazato, T., Shimizu, T., Sarukura, N., Ehrentraut, D., and Fukuda, T. (2011). Response-time-improved ZnO scintillator by impurity doping. *J. Cryst. Growth* 318, 788–790.
- Ketzer, B., Weitzel, Q., Paul, S., Sauli, F., and Ropelewski, L. (2004). Performance of triple GEM tracking detectors in the COMPASS experiment. *Nucl. Instrum Methods Phys. Res. A* 535, 314–318.
- Kim, K.S., Zhao, Y., Jang, H., Lee, S.Y., Kim, J.M., Kim, K.S., Ahn, J.-H., Kim, P., Choi, J.-Y., and

- Hong, B.H. (2009). Large-scale pattern growth of graphene films for stretchable transparent electrodes. *Nature* 457, 706.
- Kirm, M., Andrejczuk, A., Krzywinski, J., and Sobierajski, R. (2005). Influence of excitation density on luminescence decay in Y<sub>3</sub>Al<sub>5</sub>O<sub>12</sub>:Ce and BaF<sub>2</sub> crystals excited by free electron laser radiation in VUV. *Physica Status Solidi (C)* 2, 649–652.
- Kjornrattanawanich, B., Korde, R., Boyer, C.N., Holland, G.E., and Seely, J.F. (2006). Temperature dependence of the EUV responsivity of silicon photodiode detectors. *IEEE Trans. Electron Devices* 53, 218–223.
- Klason, P., Moe Børseth, T., Zhao, Q.X., Svensson, B.G., Kuznetsov, A.Y., Bergman, P.J., and Willander, M. (2008). Temperature dependence and decay times of zinc and oxygen vacancy related photoluminescence bands in zinc oxide. *Solid State Commun.* 145, 321–326.
- Kobayashi, M., Komori, J., Shimidzu, K., Izaki, M., Uesugi, K., Takeuchi, A., and Suzuki, Y. (2015). Development of vertically aligned ZnO-nanowires scintillators for high spatial resolution x-ray imaging. *Appl. Phys. Lett.* 106, 081909.
- Kogelschatz, U., Esrom, H., Zhang, J.Y., and Boyd, I.W. (2000). High-intensity sources of incoherent UV and VUV excimer radiation for low-temperature materials processing. *Appl. Surf. Sci.* 168, 29–36.
- Korde, R., and Geist, J. (1987). Quantum efficiency stability of silicon photodiodes. *Appl. Opt.* 26, 5284–5290.
- Korde, R., Prince, C., Cunningham, D., Vest, R.E., and Gullikson, E. (2003). Present status of radiometric quality silicon photodiodes. *Metrologia* 40, S145–S149.
- Kostko, O., Belau, L., Wilson, K.R., and Ahmed, M. (2008). Vacuum-Ultraviolet (VUV) photoionization of small methanol and methanol–water clusters. *J. Phys. Chem. A* 112, 9555–9562.
- Krzywinski, J., Andrejczuk, A., Bionta, R.M., Burian, T., Chalupský, J., Jurek, M., Kirm, M., Nagirnyi, V., Sobierajski, R., Tiedtke, K., et al. (2017). Saturation of the Ce:Y<sub>3</sub>Al<sub>5</sub>O<sub>12</sub> scintillator response to ultra-short pulses of extreme ultraviolet soft X-ray and X-ray laser radiation. *Opt. Mater. Express* 7, 665–675.
- Kuschnerus, P., Rabus, H., Richter, M., Scholze, F., Werner, L., and Ulm, G. (1998). Characterization of photodiodes as transfer detector standards in the 120 nm to 600 nm spectral range. *Metrologia* 35, 355–362.
- Kwok, W.M., Djurišić, A.B., Leung, Y.H., Chan, W.K., and Phillips, D.L. (2005). Time-resolved photoluminescence from ZnO nanostructures. *Appl. Phys. Lett.* 87, 223111.
- Li, J., Fan, Z.Y., Dahal, R., Nakarmi, M.L., Lin, J.Y., and Jiang, H.X. (2006). 200nm deep ultraviolet photodetectors based on AlN. *Appl. Phys. Lett.* 89, 213510.
- Li, J., Majety, S., Dahal, R., Zhao, W.P., Lin, J.Y., and Jiang, H.X. (2012). Dielectric strength, optical absorption, and deep ultraviolet detectors of hexagonal boron nitride epilayers. *Appl. Phys. Lett.* 101, 171112.
- Li, J., Nam, K.B., Nakarmi, M.L., Lin, J.Y., and Jiang, H.X. (2002). Band-edge photoluminescence of AlN epilayers. *Appl. Phys. Lett.* 81, 3365–3367.
- Li, J., Nam, K.B., Nakarmi, M.L., Lin, J.Y., Jiang, H.X., Carrier, P., and Wei, S.-H. (2003). Band structure and fundamental optical transitions in wurtzite AlN. *Appl. Phys. Lett.* 83, 5163–5165.
- Li, L., Liu, X., Pal, S., Wang, S., Ober, C.K., and Giannelis, E.P. (2017). Extreme ultraviolet resist materials for sub-7 nm patterning. *Chem. Soc. Rev.* 46, 4855–4866.
- Li, L., Wu, P., Fang, X., Zhai, T., Dai, L., Liao, M., Koide, Y., Wang, H., Bando, Y., and Golberg, D. (2010). Single-crystalline CdS nanobelts for excellent field-emitters and ultrahigh quantum-efficiency photodetectors. *Adv. Mater.* 22, 3161–3165.
- Li, X., Zhu, Y., Cai, W., Borysiak, M., Han, B., Chen, D., Piner, R.D., Colombo, L., and Ruoff, R.S. (2009). Transfer of large-area graphene films for high-performance transparent conductive electrodes. *Nano Lett.* 9, 4359–4363.
- Liao, M., Koide, Y., and Alvarez, J. (2007). Single Schottky-barrier photodiode with interdigitated-finger geometry: application to diamond. *Appl. Phys. Lett.* 90, 123507.
- Lin, C.-N., Lu, Y.-J., Yang, X., Tian, Y.-Z., Gao, C.-J., Sun, J.-L., Dong, L., Zhong, F., Hu, W.-D., and Shan, C.-X. (2018). Diamond-based all-carbon photodetectors for solar-blind imaging. *Adv. Opt. Mater.* 6, 1800068.
- Liu, H., Meng, J., Zhang, X., Chen, Y., Yin, Z., Wang, D., Wang, Y., You, J., Gao, M., and Jin, P. (2018). High-performance deep ultraviolet photodetectors based on few-layer hexagonal boron nitride. *Nanoscale* 10, 5559–5565.
- Liu, K., Dai, B., Ralchenko, V., Xia, Y., Quan, B., Zhao, J., Shu, G., Sun, M., Gao, G., Yang, L., et al. (2017). Single crystal diamond UV detector with a groove-shaped electrode structure and enhanced sensitivity. *Sens. Actuat. A Phys.* 259, 121–126.
- Liu, S., Ye, J., Cao, Y., Shen, Q., Liu, Z., Qi, L., and Guo, X. (2009). Tunable hybrid photodetectors with superhigh responsivity. *Small* 5, 2371–2376.
- Liu, Y., Gorla, C.R., Liang, S., Emanetoglu, N., Lu, Y., Shen, H., and Wraback, M. (2000). Ultraviolet detectors based on epitaxial ZnO films grown by MOCVD. *J. Electron. Mater.* 29, 69–74.
- Liu, Z., Ao, J.-P., Li, F., Wang, W., Wang, J., Zhang, J., and Wang, H.-X. (2016). Fabrication of three dimensional diamond ultraviolet photodetector through down-top method. *Appl. Phys. Lett.* 109, 153507.
- Liu, Z., Li, F., Li, S., Hu, C., Wang, W., Wang, F., Lin, F., and Wang, H. (2015). Fabrication of UV photodetector on TiO<sub>2</sub>/diamond film. *Sci. Rep.* 5, 14420.
- Lopes, T., Silva, A.L.M., Azevedo, C.D.R., Carramate, L.F.N.D., Covita, D.S., and Veloso, J.F.C.A. (2013). Position sensitive VUV gaseous photomultiplier based on Thick-multipliers with resistive line readout. *J. Instrum.* 8, P09002.
- López Paredes, B., Araújo, H.M., Froborg, F., Marangou, N., Olcina, I., Sumner, T.J., Taylor, R., Tomás, A., and Vacheret, A. (2018). Response of photomultiplier tubes to xenon scintillation light. *Astroparticle Phys.* 102, 56–66.
- McKeag, R.D., and Jackman, R.B. (1998). Diamond UV photodetectors: sensitivity and speed for visible blind applications. *Diamond Relat. Mater.* 7, 513–518.
- Meng, J.H., Zhang, X.W., Wang, H.L., Ren, X.B., Jin, C.H., Yin, Z.G., Liu, X., and Liu, H. (2015). Synthesis of in-plane and stacked graphene/hexagonal boron nitride heterostructures by combining ion beam sputtering deposition and chemical vapor deposition. *Nanoscale* 7, 16046–16053.
- Moehrs, S., del Guerra, A., Herbert, D.J., and Mandelkern, M.A. (2006). A detector head design for small-animal PET with silicon photomultipliers (SiPM). *Phys. Med. Biol.* 51, 1113–1127.
- Mohammadi, V., Golshani, N., Mok, K.R.C., de Boer, W.B., Derakhshan, J., and Nanver, L.K. (2014). Temperature dependency of the kinetics of PureB CVD deposition over patterned Si/SiO<sub>2</sub> surfaces. *Microelectron. Eng.* 125, 45–50.
- Monroy, E., Omnes, F., and Calle, F. (2003). Wide-bandgap semiconductor ultraviolet photodetectors. *Semiconductor Sci. Technol.* 18, R33.
- Moszyński, M., Ludziejewski, T., Wolski, D., Klamra, W., and Norlin, L. (1994). Properties of the YAG: Ce scintillator. *Nucl. Instrum Methods Phys. Res. A* 345, 461–467.
- Moussavi, G., Hossaini, H., Jafari, S.J., and Farokhi, M. (2014). Comparing the efficacy of UVC, UVC/ZnO and VUV processes for oxidation of organophosphate pesticides in water. *J. Photochem. Photobiol. A Chem.* 290, 86–93.
- Musienko, Y. (2009). Advances in multipixel Geiger-mode avalanche photodiodes (silicon photomultipliers). *Nucl. Instrum Methods Phys. Res. A* 598, 213–216.
- Nagayoshi, T., Kubo, H., Miuchi, K., Orito, R., Takada, A., Takeda, A., Tanimori, T., Ueno, M., Bouianov, O., and Bouianov, M. (2004). Development of μ-PIC and its imaging properties. *Nucl. Instrum Methods Phys. Res. A* 525, 20–27.
- Nakazato, T., Furukawa, Y., Tanaka, M., Tatsumi, T., Nishikino, M., Yamatani, H., Nagashima, K., Kimura, T., Murakami, H., and Saito, S. (2009). Hydrothermal-method-grown ZnO single crystal as fast EUV scintillator for future lithography. *J. Cryst. Growth* 311, 875–877.
- Nam, K.B., Li, J., Nakarmi, M.L., Lin, J.Y., and Jiang, H.X. (2003). Deep ultraviolet picosecond time-resolved photoluminescence studies of AlN epilayers. *Appl. Phys. Lett.* 82, 1694–1696.
- Nanver, L.K., Qi, L., Mohammadi, V., Mok, K.R.M., Boer, W.B.d., Golshani, N., Sammak, A., Scholtes, T.L.M., Gottwald, A., Kroth, U., et al. (2014). Robust UV/VUV/EUV PureB photodiode detector technology with high CMOS compatibility. *IEEE J. Selected Top. Quan. Electron.* 20, 306–316.
- Neutze, R., Wouts, R., van der Spoel, D., Weckert, E., and Hajdu, J. (2000). Potential for

biomolecular imaging with femtosecond X-ray pulses. *Nature* 406, 752–757.

Neves, F., Chepel, V., Akimov, D.Y., Araújo, H.M., Barnes, E.J., Belov, V.A., Burenkov, A.A., Currie, A., Edwards, B., Ghag, C., et al. (2010). Calibration of photomultiplier arrays. *Astroparticle Phys.* 33, 13–18.

Nishiura, S., Tanabe, S., Fujioka, K., and Fujimoto, Y. (2011). Properties of transparent Ce:YAG ceramic phosphors for white LED. *Opt. Mater.* 33, 688–691.

Ogasawara, K., Allegrini, F., Dayeh, M.A., Desai, M.I., Livi, S.A., Hakamata, Y., Sato, K., Ujihara, K., and Yamada, R. (2017). UV-grade silicon photomultipliers for direct counting of low-energy electrons and protons. *IEEE Trans. Nucl. Sci.* 64, 2733–2741.

Ohshima, E., Ogino, H., Niikura, I., Maeda, K., Sato, M., Ito, M., and Fukuda, T. (2004). Growth of the 2-in-size bulk ZnO single crystals by the hydrothermal method. *J. Cryst. Growth* 260, 166–170.

Onuma, T., Hazu, K., Uedono, A., Sota, T., and Chichibu, S.F. (2010). Identification of extremely radiative nature of AlN by time-resolved photoluminescence. *Appl. Phys. Lett.* 96, 061906.

Oppenländer, T. (2007). Mercury-free sources of VUV/UV radiation: application of modern excimer lamps (excilamps) for water and air treatment. *J. Environ. Eng. Sci.* 6, 253–264.

Özgür, Ü., Teke, A., Liu, C., Cho, S.-J., Morkoç, H., and Evertt, H.O. (2004). Stimulated emission and time-resolved photoluminescence in rf-sputtered ZnO thin films. *Appl. Phys. Lett.* 84, 3223–3225.

Pearson, S.J., Zolper, J.C., Shul, R.J., and Ren, F. (1999). GaN: processing, defects, and devices. *J. Appl. Phys.* 86, 1–78.

Peng, Q., Zong, N., Zhang, S., Wang, Z., Yang, F., Zhang, F., Xu, Z., and Zhou, X. (2018). DUV/VUV all-solid-state lasers: twenty years of progress and the future. *IEEE J. Selected Top. Quan. Electron.* 24, 1–12.

Pile, D.F.P. (2018). Vacuum-ultraviolet source. *Nat. Photon.* 12, 568.

Pomorski, M., Berdermann, E., Caragheorgheopol, A., Ciobanu, M., Kiš, M., Martemyanov, A., Nebel, C., and Moritz, P. (2006). Development of single-crystal CVD-diamond detectors for spectroscopy and timing. *Phys. Status Solidi* 203, 3152–3160.

Qiang, Y., Zorn, C., Barbosa, F., and Smith, E. (2013). Radiation hardness tests of SiPMs for the JLab Hall D Barrel calorimeter. *Nucl. Instrum Methods Phys. Res. A* 698, 234–241.

Qin, Y., Li, L., Zhao, X., Tompa, G.S., Dong, H., Jian, G., He, Q., Tan, P., Hou, X., Zhang, Z., et al. (2020). Metal–semiconductor–metal  $\epsilon$ -Ga<sub>2</sub>O<sub>3</sub> solar-blind photodetectors with a record-high responsivity rejection ratio and their gain mechanism. *ACS Photon.* 7, 812–820.

Qin, Y., Sun, H., Long, S., Tompa, G.S., Salagaj, T., Dong, H., He, Q., Jian, G., Liu, Q., Lv, H., et al. (2019). High-performance metal-organic chemical vapor deposition grown \$varepsilon\$-Ga<sub>2</sub>O<sub>3</sub> solar-blind photodetector with

asymmetric Schottky electrodes. *IEEE Electron. Device Lett.* 40, 1475–1478.

Remes, Z., Petersen, R., Haenen, K., Nesladek, M., and D’Olieslaeger, M. (2005). Mechanism of photoconductivity in intrinsic epitaxial CVD diamond studied by photocurrent spectroscopy and photocurrent decay measurements. *Diamond Relat. Mater.* 14, 556–560.

Rethmeier, C. (2016). Characterization of VUV sensitive SiPMs for nEXO. *J. Instrum.* 11, C03002.

Richter, M., Gottwald, A., Kroth, U., Sorokin, A.A., Bobashev, S.V., Shmaenok, L.A., Feldhaus, J., Gerth, C., Steeg, B., Tiedtke, K., et al. (2003). Measurement of gigawatt radiation pulses from a vacuum and extreme ultraviolet free-electron laser. *Appl. Phys. Lett.* 83, 2970–2972.

Richter, M., Kroth, U., Gottwald, A., Gerth, C., Tiedtke, K., Saito, T., Tassy, I., and Vogler, K. (2002). Metrology of pulsed radiation for 157-nm lithography. *Appl. Opt.* 41, 7167–7172.

Rivera, M., Velázquez, R., Aldalbahi, A., Zhou, A.F., and Feng, P. (2017). High operating temperature and low power consumption boron nitride nanosheets based broadband UV photodetector. *Scientific Rep.* 7, 42973.

Ruoff, R. (2008). Calling all chemists. *Nat. Nanotechnol.* 3, 10.

Saito, T., Hayashi, K., Ishihara, H., and Saito, I. (2006). Characterization of photoconductive diamond detectors as a candidate of FUV/VUV transfer standard detectors. *Metrologia* 43, S51.

Sajjad, M., Jadwisienczak, W.M., and Feng, P. (2014). Nanoscale structure study of boron nitride nanosheets and development of a deep-UV photo-detector. *Nanoscale* 6, 4577–4582.

Saldin, E.L., Schneidmiller, E.A., and Yurkov, M.V. (2006). Statistical properties of the radiation from VUV FEL at DESY operating at 30nm wavelength in the femtosecond regime. *Nucl. Instrum. Methods Phys. Res. A* 562, 472–486.

Samson, J.A., and Ederer, D.L. (2000). *Vacuum Ultraviolet Spectroscopy*, Vol. 32 (Academic press).

Sansone, G., Poletti, L., and Nisoli, M. (2011). High-energy attosecond light sources. *Nat. Photon.* 5, 655.

Sarubbi, F., Nanver, L.K., and Scholtes, T.L. (2006). CVD delta-doped boron surface layers for ultra-shallow junction formation. *ECS Trans.* 3, 35–44.

Sarubbi, F., Nanver, L.K., Scholtes, T.L.M., Nihtianov, S.N., and Scholze, F. (2008). Pure boron-doped photodiodes: A solution for radiation detection in EUV lithography. Paper presented at: ESSDERC 2008 - 38th European Solid-State Device Research Conference.

Schaart, D.R., van Dam, H.T., Seifert, S., Vinke, R., Dendooven, P., Löhner, H., and Beekman, F.J. (2009). A novel, SiPM-array-based, monolithic scintillator detector for PET. *Phys. Med. Biol.* 54, 3501.

Schmidtke, G., Nikutowski, B., Jacobi, C., Brunner, R., Erhardt, C., Knecht, S., Scherle, J., and Schlagenauf, J. (2014). Solar EUV irradiance measurements by the auto-calibrating EUV

spectrometers (SolACES) aboard the international space station (ISS). *Solar Phys.* 289, 1863–1883.

Schoenlein, R.W., Chattopadhyay, S., Chong, H.H.W., Glover, T.E., Heimann, P.A., Shank, C.V., Zholents, A.A., and Zolotorev, M.S. (2000). Generation of femtosecond pulses of synchrotron radiation. *Science* 287, 2237–2240.

Scholze, F., Klein, R., and Bock, T. (2003). Irradiation stability of silicon photodiodes for extreme-ultraviolet radiation. *Appl. Opt.* 42, 5621–5626.

Schreiber, S., and Faatz, B. (2015). The free-electron laser FLASH. *High Power Laser Sci. Eng.* 3, E20.

Sekiya, H., Ida, C., Kubo, H., Kurosawa, S., Tanimori, T., Yoshikawa, A., Yanagida, T., Yokota, Y., Fukuda, K., Ishizu, S., et al. (2009). Developments of a large area VUV sensitive gas PMT with GEM/μPIC. *J. Instrum.* 4, P11006.

Shaw, P.-S., Gupta, R., and Lykke, K.R. (2005). Stability of photodiodes under irradiation with a 157-nm pulsed excimer laser. *Appl. Opt.* 44, 197–207.

Shi, L., Nanver, L.K., Šakić, A., Nihtianov, S., Gottwald, A., and Kroth, U. (2010a). Optical stability investigation of high-performance silicon-based VUV photodiodes. Paper presented at: SENSORS, 2010 IEEE.

Shi, L., Sarubbi, F., Nanver, L.K., Kroth, U., Gottwald, A., and Nihtianov, S. (2010b). Optical performance of B-layer ultra-shallow-junction silicon photodiodes in the VUV spectral range. *Proced. Eng.* 5, 633–636.

Shi, L., Nihtianov, S., Nanver, L.K., and Scholze, F. (2013). Stability characterization of high-sensitivity silicon-based EUV photodiodes in a detrimental environment. *IEEE Sensors J.* 13, 1699–1707.

Shi, L., Nihtianov, S., Scholze, F., Gottwald, A., and Nanver, L.K. (2011). High-sensitivity High-Stability Silicon Photodiodes for DUV, VUV and EUV Spectral Ranges, Vol. 8145 (SPIE).

Shi, L., Nihtianov, S.N., Scholze, F., and Nanver, L.K. (2012). Electrical performance stability characterization of high-sensitivity Si-based EUV photodiodes in a harsh industrial application. Paper presented at: IECON 2012 - 38th Annual Conference on IEEE Industrial Electronics Society.

Shi, L., Sarubbi, F., Nihtianov, S.N., Nanver, L.K., Scholtes, T.L.M., and Scholze, F. (2009). High performance silicon-based extreme ultraviolet (EUV) radiation detector for industrial application. Paper presented at: 2009 35th Annual Conference of IEEE Industrial Electronics.

Shi, X., Yang, Z., Yin, S., and Zeng, H. (2016). Al plasmon-enhanced diamond solar-blind UV photodetector by coupling of plasmon and excitons. *Mater. Technol.* 31, 544–547.

Shimizu, T., Yamamoto, K., Estacio, E., Nakazato, T., Sakai, K., Sarukura, N., Ehrentraut, D., Fukuda, T., Nagasono, M., Togashi, T., et al. (2010). Response-time improved hydrothermal-method-grown ZnO scintillator for soft x-ray free-electron

- laser timing-observation. *Rev. Sci. Instr.* 81, 033102.
- Shimizu, T., Yamanoi, K., Sakai, K., Cadatal-Raduban, M., Nakazato, T., Sarukura, N., Kano, M., Wakamiya, A., Ehrentraut, D., Fukuda, T., et al. (2011). Response time-shortened zinc oxide scintillator for accurate single-shot synchronization of extreme ultraviolet free-electron laser and short-pulse laser. *Appl. Phys. Express* 4, 062701.
- Sibeck, D.G., Lopez, R.E., and Roelof, E.C. (1991). Solar wind control of the magnetopause shape, location, and motion. *J. Geophys. Res. Space Phys.* 96, 5489–5495.
- Silva, A.L.M., Azevedo, C.D.R., Carramate, L.F.N.D., Lopes, T., Castro, I.F., Oliveira, R.d., and Veloso, J.F.C.A. (2013). X-ray imaging detector based on a position sensitive THCOBRA with resistive line. *J. Instrum.* 8, P05016.
- Singh, B.K., Shefer, E., Breskin, A., Chechik, R., and Avraham, N. (2000). CsBr and CsI UV photocathodes: new results on quantum efficiency and aging. *Nucl. Instrum Methods Phys. Res. A* 454, 364–378.
- Singh, B.K., Triloki, Garg, P., Prakash, A., Di Santo, G., Nappi, E., Nitti, M.A., Valentini, A., and Zanoni, R. (2009). VUV-induced radiation ageing processes in CsI photocathodes studied by microscopy and spectroscopy techniques. *Nucl. Instrum Methods Phys. Res. A* 610, 350–353.
- Smith, B.W., and Suzuki, K. (2018). *Microlithography: Science and Technology* (CRC press).
- Solt, K., Melchior, H., Kroth, U., Kuschnerus, P., Persch, V., Rabus, H., Richter, M., and Ulm, G. (1996). PtSi-n-Si Schottky-barrier photodetectors with stable spectral responsivity in the 120–250 nm spectral range. *Appl. Phys. Lett.* 69, 3662–3664.
- Soltani, A., Barkad, H.A., Mattalah, M., Benbakhti, B., Jaeger, J.-C.D., Chong, Y.M., Zou, Y.S., Zhang, W.J., Lee, S.T., BenMousa, A., et al. (2008). 193nm deep-ultraviolet solar-blind cubic boron nitride based photodetectors. *Appl. Phys. Lett.* 92, 053501.
- Sorokin, A.A., Bican, Y., Bonfigt, S., Brachmanski, M., Braune, M., Jastrow, U.F., Gottwald, A., Kaser, H., Richter, M., and Tiedke, K. (2019). An X-ray gas monitor for free-electron lasersThis article will form part of a virtual special issue containing papers presented at the PhotonDiag2018 workshop. *J. Synchrotron Radiat.* 26, 1092–1100.
- Sorokin, A.A., Bobashev, S.V., Feldhaus, J., Gerth, C., Gottwald, A., Hahn, U., Kroth, U., Richter, M., Shnaenok, L.A., Steeg, B., et al. (2004). Gas-monitor detector for intense and pulsed VUV/EUV free-electron laser radiation. *AIP Conf. Proc.* 705, 557–560.
- Sul, W., Lee, C., and Cho, G. (2013). Influence of guard-ring structure on the dark count rates of silicon photomultipliers. *IEEE Electron. Device Lett.* 34, 336–338.
- Sun, H., Li, K.-H., Castanedo, C.G.T., Okur, S., Tompa, G.S., Salagaj, T., Lopatin, S., Genovese, A., and Li, X. (2018). HCl flow-induced phase change of  $\alpha$ ,  $\beta$ , and  $\epsilon$ -Ga<sub>2</sub>O<sub>3</sub> films grown by MoCVD. *Cryst. Growth Des.* 18, 2370–2376.
- Sun, X.-Y., Gao, P., Wu, S., Wu, H.-S., Hu, Q.-L., Zhang, X., Huang, Y., and Tao, Y. (2015). Luminescent properties and energy transfer of Ce<sup>3+</sup>-activated Li<sub>2</sub>O-B<sub>2</sub>O<sub>3</sub>-Gd<sub>2</sub>O<sub>3</sub> scintillating glasses under VUV-UV and X-ray excitation. *Nucl. Instrum Methods Phys. Res. B* 350, 36–40.
- Suzuki, K., Cadatal-Raduban, M., Kase, M., and Ono, S. (2019). Band gap engineering of Ca<sub>x</sub>Sr<sub>1-x</sub>F<sub>2</sub> and its application as filterless vacuum ultraviolet photodetectors with controllable spectral responses. *Opt. Mater.* 88, 576–579.
- Takada, A., Hattori, K., Kabuki, S., Kubo, H., Miuchi, K., Nagayoshi, T., Nishimura, H., Okada, Y., Orito, R., and Sekiya, H. (2007). A very large area Micro Pixel Chamber. *Nucl. Instrum Methods Phys. Res. A* 573, 195–199.
- Tanaka, M., Nishikino, M., Yamatani, H., Nagashima, K., Kimura, T., Furukawa, Y., Murakami, H., Saito, S., Sarukura, N., Nishimura, H., et al. (2007). Hydrothermal method grown large-sized zinc oxide single crystal as fast scintillator for future extreme ultraviolet lithography. *Appl. Phys. Lett.* 91, 231117.
- Tang, Y., Zhou, S., Chen, C., Yi, X., Feng, Y., Lin, H., and Zhang, S. (2015). Composite phase ceramic phosphor of Al<sub>2</sub>O<sub>3</sub>-Ce:YAG for high efficiency light emitting. *Opt. Express* 23, 17923–17928.
- Teraji, T., Yoshizaki, S., Wada, H., Hamada, M., and Ito, T. (2004). Highly sensitive UV photodetectors fabricated using high-quality single-crystalline CVD diamond films. *Diamond Relat. Mater.* 13, 858–862.
- Tiedke, K., Braune, M., Brenner, G., Dziarzhyski, S., Faatz, B., Feldhaus, J., Keitel, B., Kuhn, H., Kuhlmann, M., and Plonjes, E. (2013). Challenges for Detection of Highly Intense FEL Radiation: Photon Beam Diagnostics at FLASH1 and FLASH2. Paper presented at: Proc 35th Free-Electron Laser Conf.
- Tiedke, K., Feldhaus, J., Hahn, U., Jastrow, U., Nunez, T., Tschentscher, T., Bobashev, S.V., Sorokin, A.A., Hastings, J.B., Möller, S., et al. (2008). Gas detectors for x-ray lasers. *J. Appl. Phys.* 103, 094511.
- Tremsin, A.S., and Siegmund, O.H.W. (2000). Heat enhancement of radiation resistivity of evaporated CsI, KI and KBr photocathodes. *Nucl. Instrum Methods Phys. Res. A* 442, 337–341.
- Tsai, D.-S., Lien, W.-C., Lien, D.-H., Chen, K.-M., Tsai, M.-L., Senesky, D.G., Yu, Y.-C., Pisano, A.P., and He, J.-H. (2013). Solar-blind photodetectors for harsh electronics. *Sci. Rep.* 3, 2628.
- Tsao, J.Y., Chowdhury, S., Hollis, M.A., Jena, D., Johnson, N.M., Jones, K.A., Kaplar, R.J., Rajan, S., Van de Walle, C.G., Bellotti, E., et al. (2018). Ultrawide-bandgap semiconductors: research opportunities and challenges. *Adv. Electron. Mater.* 4, 1600501.
- Vartsky, D., Roy, A., Coimbra, A., Shchemelinin, S., Israelashvili, I., Arazi, L., Erdal, E., and Breskin, A. (2019). CsI-photocathode in-situ monitoring system in gaseous and noble-liquid photomultipliers. *J. Instrum.* 14, T07006.
- Wabnitz, H., Bittner, L., de Castro, A.R.B., Döhrmann, R., Gürler, P., Laermann, T., Laasch, W., Schulz, J., Swiderski, A., von Haeften, K., et al. (2002). Multiple ionization of atom clusters by intense soft X-rays from a free-electron laser. *Nature* 420, 482–485.
- Wang, H., Zhang, X., Liu, H., Yin, Z., Meng, J., Xia, J., Meng, X.-M., Wu, J., and You, J. (2015). Synthesis of large-sized single-crystal hexagonal boron nitride domains on nickel foils by ion beam sputtering deposition. *Adv. Mater.* 27, 8109–8115.
- Wang, J., Ma, F., Liang, W., and Sun, M. (2017). Electrical properties and applications of graphene, hexagonal boron nitride (h-BN), and graphene/h-BN heterostructures. *Mater. Today Phys.* 2, 6–34.
- Wei, T., Islam, S., Jahn, U., Yan, J., Lee, K., Bharadwaj, S., Ji, X., Wang, J., Li, J., and Protasenko, V.J.O.L. (2020). GaN/AlN quantum-disk nanorod 280 nm deep ultraviolet light emitting diodes by molecular beam epitaxy. *Opt. Lett.* 45, 121–124.
- Wellhöfer, M., Hoeft, J.T., Martins, M., Wurth, W., Braune, M., Viehaus, J., Tiedke, K., and Richter, M. (2008). Photoelectron spectroscopy as a non-invasive method to monitor SASE-FEL spectra. *J. Instrum.* 3, P02003.
- Winick, H., and Doniach, S. (2012). *Synchrotron Radiation Research* (Springer Science & Business Media).
- Wojtowicz, A.J. (2002). Rare-earth-activated wide bandgap materials for scintillators. *Nucl. Instrum Methods Phys. Res. A* 486, 201–207.
- Wojtowicz, A.J., Drozdowski, W., Wisniewski, D., Lefaucheur, J.-L., Galazka, Z., Gou, Z., Lukasiewicz, T., and Kisielewski, J. (2006). Scintillation properties of selected oxide monocrystals activated with Ce and Pr. *Opt. Mater.* 28, 85–93.
- Wojtowicz, A.J., Szupryczynski, P., Glodo, J., Drozdowski, W., and Wisniewski, D. (2000). Radioluminescence and recombination processes in BaF<sub>2</sub>: Ce. *J. Phys. Condensed Matter* 12, 4097.
- Xie, W., Fu, Y., Li, Y., Li, J., Li, Y., and Yue, Q. (2015). Cryogenic THGEM-GPM for the readout of scintillation light from liquid argon. *Nucl. Instrum Methods Phys. Res. A* 774, 120–126.
- Xie, Y., Liu, H., Zhang, A., Liu, Y., Hu, T., Zhou, L., An, Z., Cai, X., Fang, J., Ge, Y., et al. (2012). Quantum efficiency measurement of CsI photocathodes using synchrotron radiation at BSRF. *Nucl. Instrum Methods Phys. Res. A* 664, 310–316.
- Xin, X., Yan, F., Koeth, T.W., Joseph, C., Hu, J., Wu, J., and Zhao, J.H. (2005). Demonstration of 4H-SiC visible-blind EUV and UV detector with large detection area. In *Electronics Letters* (Institution of Engineering and Technology), pp. 1192–1193.
- Xu, C., Du, Z., Huang, Y., Dong, M., Lin, R., Li, Y., Wang, B., Zheng, W., and Huang, F. (2018a). Amorphous-MgGaO film combined with graphene for vacuum-ultraviolet photovoltaic detector. *ACS Appl. Mater. Interfaces* 10, 42681–42687.
- Xu, M., Chen, L., Liu, B., Zhu, Z., Huang, F., Zheng, W., He, C., and Ouyang, X. (2018b). Effects of

photonic crystal structures on the imaging properties of a ZnO:Ga image converter. *Opt. Lett.* 43, 5647–5650.

Yamanoi, K., Shimizu, T., Furukawa, Y., Cadatal-Raduban, M., Nakazato, T., Sakai, K., Tsuboi, M., Nishi, R., Sarukura, N., Tanaka, M., et al. (2013). Optical properties of hydrothermal-method-grown ZnO crystal as EUV laser diagnostics material. *J. Cryst. Growth* 362, 264–267.

Yamazaki, R., Suzuki, K., Otani, S., and Ono, S. (2017). Controlling laser power irradiation of pulsed laser deposition for fabricating high resistivity NdF<sub>3</sub> thin film. Paper presented at: 2017 Conference on Lasers and Electro-Optics Pacific Rim (CLEO-PR).

Yoder, M.N. (1996). Wide bandgap semiconductor materials and devices. *IEEE Trans. Electron Devices* 43, 1633–1636.

Yu, C., and Wang, H. (2010). Large lateral photovoltaic effect in metal-(oxide)-semiconductor structures. *Sensors* 10, 10155–10180.

Zabrodskii, V., Aruev, P., Belik, V., Ber, B., Filimonov, V., Kholupenko, E., Kirilenko, D., Krassilchitskikh, A., Nikolaev, A., Sherstnev, E., et al. (2015). SiPM prototype for direct VUV registration. *Nucl. Instrum Methods Phys. Res. A* 787, 348–352.

Zhang, J.P., Chitnis, A., Adivarahan, V., Wu, S., Mandavilli, V., Pachipulusu, R., Shatalov, M., Simin, G., Yang, J.W., and Khan, M.A. (2002). Milliwatt power deep ultraviolet light-emitting diodes over sapphire with emission at 278 nm. *Appl. Phys. Lett.* 81, 4910–4912.

Zhang, W.J., Chan, C.Y., Meng, X.M., Fung, M.K., Bello, I., Lifshitz, Y., Lee, S.T., and Jiang, X. (2005a). The mechanism of chemical vapor deposition of cubic boron nitride films from fluorine-containing species. *Angew. Chem. Int. Ed.* 44, 4749–4753.

Zhang, W.J., Meng, X.M., Chan, C.Y., Chan, K.M., Wu, Y., Bello, I., and Lee, S.T. (2005b). Interfacial study of cubic boron nitride films deposited on diamond. *J. Phys. Chem. B* 109, 16005–16010.

Zhang, X., Zhang, Y., Qian, Y., Feng, C., Zhang, J., Jiang, Y., and Pan, Z. (2017). Spectral response characteristics of transmission-mode alkali telluride photocathodes working from vacuum-ultraviolet to ultraviolet band. *J. Vac. Sci. Technol. B* 35, 061202.

Zheng, W., Huang, F., Zheng, R., and Wu, H. (2015). Low-dimensional structure vacuum-ultraviolet-sensitive ( $\lambda < 200$  nm) photodetector with fast-response speed based on high-quality AlN micro/nanowire. *Adv. Mater.* 27, 3921–3927.

Zheng, W., Lin, R., Jia, L., and Huang, F. (2019a). Vacuum-ultraviolet-oriented van der Waals photovoltaics. *ACS Photonics* 6, 1869–1875.

Zheng, W., Lin, R., Jia, L., and Huang, F. (2019b). Vacuum ultraviolet photovoltaic arrays. *Photon. Res.* 7, 98–102.

Zheng, W., Lin, R., Ran, J., Zhang, Z., Ji, X., and Huang, F. (2018a). Vacuum-ultraviolet photovoltaic detector. *ACS Nano* 12, 425–431.

Zheng, W., Lin, R., Zhang, D., Jia, L., Ji, X., and Huang, F. (2018b). Vacuum-ultraviolet photovoltaic detector with improved response speed and responsivity via heating annihilation trap state mechanism. *Adv. Opt. Mater.* 6, 1800697.

Zheng, W., Lin, R., Zhang, Z., and Huang, F. (2018c). Vacuum-ultraviolet photodetection in few-layered h-BN. *ACS Appl. Mater. Interfaces* 10, 27116–27123.

Zheng, W., Lin, R., Zhu, Y., Zhang, Z., Ji, X., and Huang, F. (2018d). Vacuum ultraviolet photodetection in two-dimensional oxides. *ACS Appl. Mater. Interfaces* 10, 20696–20702.

Zhou, A.F., Aldalbahi, A., and Feng, P. (2016). Vertical metal-semiconductor-metal deep UV photodetectors based on hexagonal boron nitride nanosheets prepared by laser plasma deposition. *Opt. Mater. Express* 6, 3286–3292.